A Glucagon-Like Peptide-1 Analog Reverses the Molecular Pathology and Cardiac Dysfunction of a Mouse Model of Obesity

Mohammad Hossein Noyan-Ashraf, PhD; Eric Akihiko Shikatani, MSc; Irmgard Schuiki, PhD; Ilya Mukovozov, MSc; Jun Wu, MD, MSc; Ren-Ke Li, MD, PhD; Allen Volchuk, PhD; Lisa Annette Robinson, MD; Filio Billia, MD, PhD; Daniel J. Drucker, MD*; Mansoor Husain, MD*

Background—Cardiac consequences of obesity include inflammation, hypertrophy, and compromised energy metabolism. Glucagon-like peptide-1 is an incretin hormone capable of cytoprotective actions that reduces inflammation and endoplasmic reticulum stress in other tissues. Here we examine the cardiac effects of the glucagon-like peptide-1 analog liraglutide in a model of obesity, independent of changes in body weight.

Methods and Results—C57Bl6 mice were placed on a 45% high-fat diet (HFD) or a regular chow diet. Mice on HFD developed 46±2% and 60±2% greater body weight relative to regular chow diet–fed mice at 16 and 32 weeks, respectively (both $P<0.0001$), manifesting impaired glucose tolerance, insulin resistance, and cardiac ceramide accumulation by 16 weeks. One-week treatment with liraglutide (30 μg/kg twice daily) did not reduce body weight, but reversed insulin resistance, cardiac tumor necrosis factor-α expression, nuclear factor kappa B translocation, obesity-induced perturbations in cardiac endothelial nitric oxide synthase, connexin-43, and markers of hypertrophy and fibrosis, in comparison with placebo-treated HFD controls. Liraglutide improved the cardiac endoplasmic reticulum stress response and also improved cardiac function in animals on HFD by an AMP-activated protein kinase–dependent mechanism. Supporting a direct mechanism of action, liraglutide (100 nmol/L) prevented palmitate-induced lipotoxicity in isolated mouse cardiomyocytes and primary human coronary smooth muscle cells and prevented adhesion of human monocytes to tumor necrosis factor-α–activated human endothelial cells in vitro.

Conclusions—Weight-neutral treatment with a glucagon-like peptide-1 analog activates several cardioprotective pathways, prevents HFD-induced insulin resistance and inflammation, reduces monocyte vascular adhesion, and improves cardiac function in vivo by activating AMP-activated protein kinase. These data support a role for glucagon-like peptide-1 analogs in limiting the cardiovascular risks of obesity. **(*Circulation*. 2013;127:74-85.)**

Key Words: obesity ■ heart ■ glucagon-like peptide-1 ■ inflammation ■ connexin-43 ■ AMP-activated protein kinase

Obesity is an emerging pandemic linked to type 2 diabetes mellitus, hypertension, and cardiovascular disease.[1] Putative mechanisms underlying these associations include insulin resistance, cardiac hypertrophy, and compromised myocardial contractile function and energy metabolism both in rodents and humans.[2] Besides shifting energy balance, which alters metabolic regulation, models of obesity have also been associated with low-grade inflammation and endoplasmic reticulum (ER) stress in several organs, including the heart.[3,4] Importantly, the ER stress–induced unfolded protein response intersects with inflammatory signals to contribute to insulin resistance in liver, fat, and skeletal muscle.[5]

Clinical Perspective on p 85

Mice on a high-fat diet (HFD) have been used to replicate these and other features of human obesity.[6] HFD-induced obesity in mice is associated with several adverse cardiac effects including inflammation, hypertrophy, fibrosis, apoptosis, and contractile dysfunction, depending on the dietary lipid composition, duration, and percentage of caloric intake.[2] In addition, diet-induced obesity may result in insulin resistance and reduced cardiac glucose uptake.[4] Furthermore, obesity-induced inflammation also contributes to the pathogenesis of diabetes mellitus and obesity-associated heart disease.

Received January 5, 2012; accepted November 16, 2012

From the Toronto General Research Institute, Toronto, Canada (M.H.N.-A., E.A.S., I.S., J.W., R.-K.L., A.V., F.B., M.H.); Hospital for Sick Children, Toronto, Canada (I.M., L.A.R.); Samuel Lunenfeld Research Institute, Toronto Canada (D.J.D.); Heart & Stroke Richard Lewar Centre of Excellence, University of Toronto, Toronto, Canada (D.J.D., M.H.).

*These senior authors contributed equally to this study.

The online-only Data Supplement is available with this article at http://circ.ahajournals.org/lookup/suppl/doi:10.1161/CIRCULATIONAHA.112.091215/-/DC1.

Correspondence to Mansoor Husain, MD, Heart & Stroke Richard Lewar Centre of Excellence, University of Toronto, Toronto General Research Institute, 200 Elizabeth St, TMDT3-909 Toronto, ON, Canada M6C-3J9. E-mail mansoor.husain@utoronto.ca

Circulation **is available at http://circ.ahajournals.org** **DOI: 10.1161/CIRCULATIONAHA.112.091215**

For example, neutralizing the inflammatory mediator tumor necrosis factor-α (TNF-α) in rats can ameliorate insulin resistance,[7] and mice with the genetic absence of TNF-α or TNF-α receptor-1 are protected from insulin resistance induced by diet or a genetic model of obesity.[8] Finally, clinical studies suggest that the inflammation associated with obesity is an independent predictor of heart failure.[9] More recently, the diet-independent *ob/ob* mouse model of obesity was shown to manifest myocardial ER stress in concert with contractile dysfunction.[10] Together, these and other epidemiological data linking inflammatory and ER-stress signaling with cardiac dysfunction,[11] provide a rationale for therapeutic targeting of these pathways in obesity-induced heart disease.

Glucagon-like peptide-1 (GLP-1) is an incretin hormone that regulates glucose metabolism and may attenuate insulin resistance. This peptide and its analogs also exert cytoprotective actions,[12] with GLP-1 receptor (GLP-1R) activation resulting in reduced inflammation in atherosclerotic lesions,[13] brain,[14] and pancreatic β-cells.[15] Of particular interest, GLP-1R agonists also induce moderate weight loss through multiple mechanisms, including appetite suppression, delayed gastric emptying, and increased energy expenditure.[16] For example, liraglutide, an approved treatment for type 2 diabetes mellitus that shares considerable amino acid homology with human GLP-1, is being tested for its ability to reduce body weight in obese adults.[17] Nevertheless, few data exist on the effects of liraglutide in preclinical models of obesity.[18] In a recent study examining hepatic steatosis after only 8 weeks of a HFD, Mells et al[18] showed that 4 weeks of treatment with a weight loss–inducing dose of liraglutide (200 μg/kg daily) reversed obesity-induced increases in blood pressure and cardiac hypertrophy, without describing cardiac histology, cardiac function, or any underlying mechanisms. Although the ability of drugs targeting the GLP-1/GLP-1R axis to affect ER stress, unfolded protein response, and autophagy in the liver have also recently been described,[19] the role, if any, of these molecular mechanisms in the pathophysiology of obesity-associated heart disease has not been examined.

Considerable evidence demonstrates that GLP-1 and related peptides protect the isolated mouse heart against ischemia-reperfusion injury[20] and protect cardiomyocytes and endothelial cells from oxidative stress and hypoxia-reoxygenation.[21] Moreover, pretreatment with liraglutide reduces cardiac rupture and adverse ventricular remodeling following myocardial infarction in mice.[22] Accordingly, we hypothesized that sustained GLP-1R activation may also prove beneficial in a mouse model of obesity-induced heart disease. Here, we show in both early (16 week) and late (32 week) stages of HFD-induced obesity and heart disease, that treatment for only 7 days with a weight-neutral dose of liraglutide affects cardiac markers of ER homeostasis and reduces markers of inflammation, with an AMP-activated protein kinase (AMPK)–dependent improvement of cardiac function in vivo. These findings were accompanied by rescue of HFD-induced loss of AMPK, extracellular-signal–regulated kinase (ERK)1/2, and glycogen synthase kinase 3β (GSK-3β) signaling, and correction of obesity-induced decreases in endothelial nitric oxide synthase (eNOS), and the cardiac gap junction protein, connexin-43. Liraglutide also reversed HFD-induced increases in cardiac levels of TNF-α, nuclear translocation of nuclear factor kappa B (NFκB), expression of procollagen 1A1, and perivascular fibrosis. To examine if these effects are due to direct cardiac actions of the GLP-1R agonist, we also show that liraglutide protects isolated mouse neonatal cardiomyocytes and human coronary smooth muscle cells from palmitate-induced lipotoxicity and prevents TNF-α–induced endothelial cell–macrophage interactions in human cell lines. Together, these data support the notion that GLP-1R activation may produce salutary effects in obesity-induced heart disease.

Materials and Methods

Animals

Protocols were approved by our institution in accordance with guidelines of the Canadian Council for Animal Care. Male 10- to 12-week-old C57BL/6 mice were obtained from Jackson Labs and housed for ≥2 weeks before experimentation.

Diet and Drug Treatment

Twelve- to 14-week-old mice were fed HFD (45% calories from fat, diet D12451; Research Diets Inc) or RD (regular chow diet) for 16, 20, or 32 weeks with only the final week of each duration including a 7-day treatment with a weight-neutral dose of liraglutide (30 μg/kg SC BID) or placebo (phosphate-buffered saline 100 μL SC BID). To seek evidence for ER stress, a small number of mice were maintained on HFD and RD for 56 weeks. Body weights were recorded before and after each treatment. The experimental schema is shown in Figure 1.

Online-only Data Supplement

The online-only Data Supplement provides details regarding blood biochemistry, including fasting blood glucose, triglyceride, and cholesterol levels. Histology and morphometry are also described. Online-only Data Supplement Table I lists all antibodies used. Detailed methods for in vivo assessments of cardiac structure, hypertrophy, and function, including echocardiography and invasive hemodynamics, are provided. Assays for cell adhesion, lipotoxicity, X-box binding protein 1 (XBP1) splicing, apoptosis, and metabolic testing, including the intraperitoneal glucose tolerance test and in vivo insulin sensitivity, are also described.

Statistical Analyses

Data are expressed as mean±SE using GraphPad Prism version 5.04 for Windows (GraphPad Software, CA). Significance was defined as 2-sided $P<0.05$. For analysis of Western blot densitometry, pressure volume loops, echocardiography, blood biochemistry, real-time polymerase chain reaction data, adhesion, and sodium 2,3,-bis(2-methoxy-4-nitro-5-sulfophenyl)-5-[(phenylamino)-carbonyl]-2H-tetrazolium inner salt (XTT) assays, a 1-way analysis of variance with the Tukey post hoc test was used to evaluate differences between groups. Changes in blood glucose concentrations over time during the intraperitoneal glucose tolerance test were analyzed between each treatment group by 2-way repeated-measures analysis of variance with the Bonferroni-Dunn post hoc test. For other comparisons between 2 groups, we used paired or unpaired 2-tailed Student *t* tests as appropriate. The nonparametric Wilcoxon rank sum test was used for comparison of 2 groups with smaller sample size (ie, n=3–4/group).

Results

A Weight-Neutral Dose of Liraglutide Lowered Fasting Blood Glucose Levels

Mice fed a HFD became markedly obese, with 46±2%, 53±1%, 60±2%, and 114±3% increases in body weight (BW) at the 16-, 20-, 32-, and 56-week time points, respectively ($P<0.001$

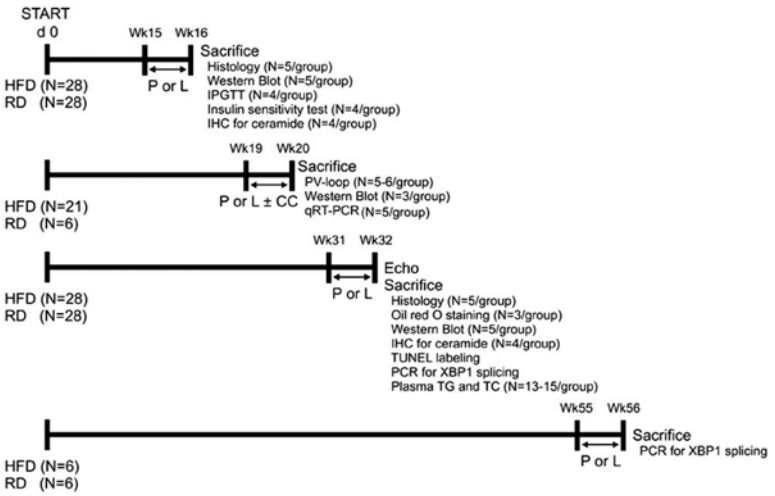

Figure 1. Schematic of animal experimentation in vivo. The 4 experimental periods (16, 20, 32, and 56 weeks) of high-fat diet (HFD) versus regular diet (RD) are shown. Each involved only 1 week of treatment with liraglutide (L: 30 μg/kg SC BID) or placebo (P: equal volume of 100 μL of PBS SC BID). CC indicates compound C; IHC, immunohistochemistry; IPGTT, intraperitoneal glucose tolerance test; PBS, phosphate-buffered saline; PCR, polymerase chain reaction; PV, pressure volume; TC, total cholesterol; TG, triglyceride; and TUNEL, terminal deoxynucleotidyl transferase-mediated dUTP nick end-labeling.

for each comparison; see online-only Data Supplement Table II for absolute values). Treatment with liraglutide (30 μg/kg SC BID) for 1 week did not induce weight loss in RD- or HFD-fed mice at these same time points (online-only Data Supplement Table II). Although chosen to be weight neutral, the dose of liraglutide administered did demonstrate biological activity, with reductions in fasting blood glucose observed in lean and obese groups (online-only Data Supplement Table II).

Obese Mice Manifest Impaired Glucose Handling, Insulin Resistance, Hypercholesterolemia, and Cardiac Lipid Accumulation

The intraperitoneal glucose tolerance test demonstrated glucose intolerance in HFD-fed mice at 16 weeks, which was corrected by liraglutide (Figure 2A). At this stage, insulin-induced phosphorylation of Akt (same as protein kinase B) in both liver and heart were reduced in obese animals (Figure 2B), suggesting insulin resistance. Treatment with liraglutide for 1 week improved all insulin-activated signals examined in the hearts and livers of mice on HFD in comparison with placebo-treated HFD-fed controls, including IRS1, Akt, GSK3β, and ERK1/2 (Figure 2C). Obesity also caused reduced total cardiac levels of the glucose transporter GLUT4 and impaired insulin-induced membrane translocation of GLUT4 (Figure 2D). Liraglutide normalized both of these abnormalities (Figure 2D). Our model also generated significantly increased plasma total cholesterol concentrations, which were partially alleviated by 1-week treatment with liraglutide (Figure 2E). Although no elevations in plasma triglyceride levels were observed at this stage (Figure 2E), qualitative and quantitative immunohistochemistry demonstrated cardiac accumulation of the sphingolipid ceramide (Figure 3E–H), and neutral lipids, as well, as determined by oil red O staining (Figure 3I–J).

HFD for 16 Weeks Did Not Affect Cardiac Structure

Despite the above metabolic perturbations and significant increases in body weight (RD, 25.7±0.6 versus HFD, 44.4±1.3 g, $P<0.0001$, n=18/group), heart weight at 16 weeks did not differ between RD- and HFD-fed mice (122.6±3.1 versus 122.2±6.7 mg, P=NS), with the fall in the heart weight/BW ratio (RD: 4.1 ± 0.1 versus HFD: 2.6±0.1; $P<0.0001$) in obese mice driven exclusively by their gain in BW. Confirming the absence of cardiac hypertrophy at this time point, no differences in morphometry-defined cardiomyocyte size or histology-defined perivascular and intermyofibrillar fibrosis were observed between RD- and HFD-fed animals (online-only Data Supplement Figure IA and IB).

Liraglutide Corrected HFD-Induced Abnormalities in Cardiac Signaling

Levels of the metabolic sensing/modulator protein–phosphorylated AMPK were reduced in the hearts of mice on a HFD for 16 and 32 weeks. This abnormality was more than reversed by 1 week of treatment with liraglutide (Figure 4A). Curiously, liraglutide did not increase phosphorylation of the survival kinase Akt in the hearts of mice on HFD for 32 weeks (Figure 4B), as it did in the hearts of mice on HFD for 16 weeks (Figure 2C), lean mice (online-only Data Supplement Figure IIA), or in previous studies of mice undergoing myocardial infarction.[22] However, liraglutide effectively normalized or increased phosphorylation of other important signaling molecules such as GSK-3β and ERK1/2 in the hearts of obese mice at this later stage (Figure 4C and D). Suggesting selective pathogenesis, neither obesity nor liraglutide had any effect on phosphorylation of the cardiac signaling molecules p38 mitogen-activated protein kinase (Figure 4E) or mammalian target of rapamycin (Figure 4F).

HFD and Liraglutide Influenced Cardiac ER Homeostasis

To seek definitive evidence of ER stress in the heart, we first examined cardiac mRNA for the presence of spliced XBP1. Consistent with a report showing that HFD did not increase spliced XBP1 levels in islets,[23] we failed to detect spliced XBP1 in the hearts of mice on HFD for 32 weeks (online-only Data Supplement Figure II). In a small group of mice maintained on HFD for 56 weeks (n=3/group) and found to have severe hepatic steatosis (online-only Data Supplement Figure II), we still did not find evidence of XBP1 splicing in heart or liver (Figure 5A). However, protein levels of several ER-stress markers, including the ER chaperones glucose-regulated protein, disulfide isomerase, and phosphorylation of eukaryotic translation initiation factor 2α were increased in cardiac extracts of obese mice fed HFD for 32 weeks (Figure 5B), suggesting

HFD-induced accumulation of misfolded proteins in the ER. Unexpectedly, liraglutide enhanced expression levels of these ER markers in obese hearts at both the 16- (online-only Data Supplement Figure II) and 32-week time points (Figure 5B).

Liraglutide Reversed Obesity-Induced Abnormalities in Cardiac Gene Expression and Fibrosis

To explore the molecular and structural basis of our model, we used gene expression and immunohistochemistry analyses. Both cardiac fibrosis and adverse remodeling of gap junction proteins are known to participate in the pathogenesis of cardiac dysfunction, including models of inflammation, obesity, and diabetes mellitus.[24,25] Indeed, gap junction remodeling precedes contractile dysfunction in an inducible transgene model of inflammatory cardiomyopathy.[26] Here, we identify these mechanisms as targets amenable to GLP-1R activation. Liraglutide treatment of obese mice for 1 week restored diminished and disorganized expression of cardiac connexin-43 (Cx-43) (Figure 6A through 6D), reversed the down-regulated levels of cardiac eNOS (Figure 5E), and reduced upregulated levels of procollagen 1A1 and perivascular fibrosis, as determined by Western blot and polarized microscopy (Figure 6F and G).

Neither HFD Nor Liraglutide Altered Expression Levels of Mitochondrial Markers in the Heart

Obesity is associated with reduced mitochondrial biogenesis and decreased expression of mitochondrial proteins in fat and skeletal muscle of obese rodents.[27] As such, we analyzed protein abundance of selected markers of mitochondrial biogenesis (peroxisome proliferator-activated receptor-γ coactivator-1α) and cell respiration (cytochrome c and cytochrome c oxidase IV) in the hearts of our various experimental groups. Levels of peroxisome proliferator-activated receptor-γ coactivator-1α, cytochrome c, and cytochrome c oxidase IV did not change in any group (online-only Data Supplement Figure II).

Liraglutide Reduced Inflammation in the Hearts of HFD-Fed Mice

In contrast to the absence of altered mitochondrial markers, the hearts of HFD-fed mice manifested increased expression of the inflammatory cytokine TNF-α and increased activation

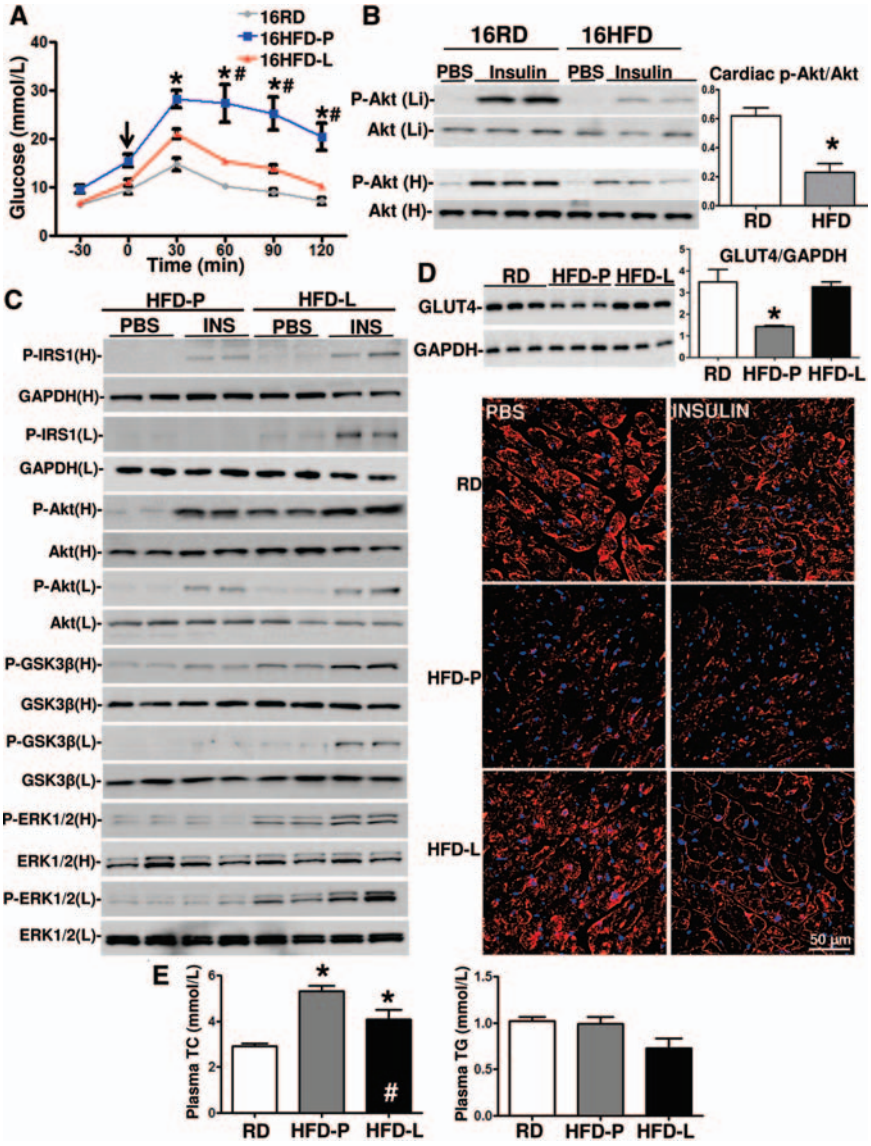

Figure 2. Characterization of HFD-induced obesity model. **A,** HFD impaired glucose tolerance. After a 6-hour fast, serial tail blood glucose measurements were made before and after glucose administration (arrow, 1 g/kg IP). Obese (16HFD-P) mice showed elevated blood glucose levels versus lean controls (16RD), and versus obese mice treated with liraglutide (HFD-L) by 2-way repeated-measures ANOVA with Bonferroni-Dunn post hoc test: **P*<0.0001 for HFD-P versus RD; #*P*<0.001 for HFD-P versus HFD-L, n=4/group. **B**, Insulin sensitivity in vivo was assessed by measuring insulin-induced phosphorylation of Akt (P-Akt) in cardiac tissues following an overnight fast. Heart (H) and liver (Li) extracts from PBS-treated mice served as negative controls revealing background levels of P-Akt. Insulin resulted in diminished P-Akt levels in HFD- versus RD-fed mice, **P*<0.05 by nonparametric Wilcoxon rank sum test (n=3/group). **C**, Insulin sensitivity in cardiac and hepatic protein extracts. Liraglutide corrected the impaired insulin-induced phosphorylation of downstream targets IRS1, Akt, GSK3β, and ERK1/2 in HFD-fed mice. **D**, HFD resulted in reduced cardiac GLUT4 levels, 1-way ANOVA: **P*<0.05 by Tukey multiple comparison post hoc test, n=3 group). Confocal microscopy revealed improved insulin-induced membrane translocation of GLUT4 in cardiomyocytes of obese (16HFD) mice treated with liraglutide. **E**, Obese (16HFD) mice have increased plasma total cholesterol (TC), but not triglyceride (TG) concentrations. TC, 1-way ANOVA: **P*<0.0001 versus RD, #*P*<0.05 versus HFD-P by Tukey multiple comparison post hoc test; TG, *P*=NS; n=4–5/group. ANOVA indicates analysis of variance; HFD, high-fat diet; INS, insulin; NS, not significant; PBS, phosphate-buffered saline; and RD, regular diet.

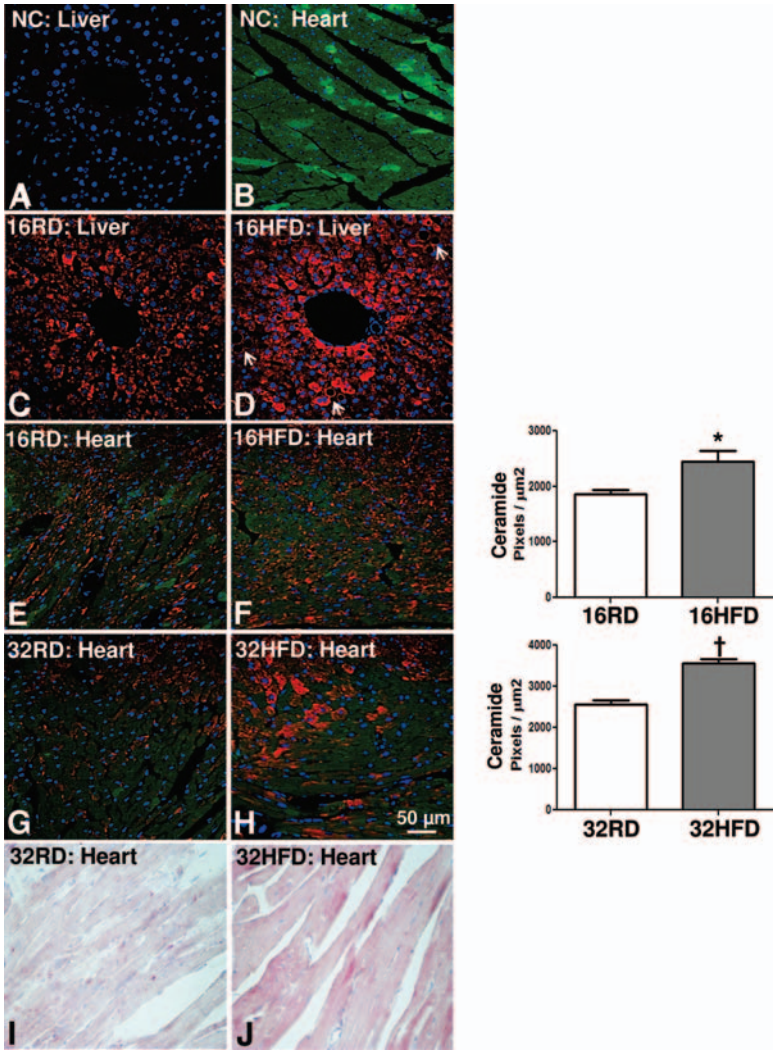

Figure 3. HFD-induced obesity causes increased cardiac lipid accumulation. Tissue levels of the sphingolipid ceramide were quantified in liver and heart by immunohistochemical staining, confocal microscopy, and digital image analysis. Sections of liver (**A**) and heart (**B**) in which the 1°anticeramide Ab was omitted served as negative controls for nonspecific background staining by the 2°Ab (red). Ab against cardiac troponin-I (TnIc) and Hoechst were used to label cardiac myocytes (green) and nuclei (blue), respectively. Quantitative analysis of signal intensity revealed increased hepatic (**C, D**) and cardiac ceramide levels after 16 (**E, F**) and 32 (**G, H**) weeks of HFD. Oil red O staining also revealed increased cardiac accumulation of neutral lipids after 32 weeks of HFD (**I, J**); **P*<0.05, †*P*<0.01 by nonparametric Wilcoxon rank sum test, n=4 mice/group. Ab indicates antibody; HFD, high-fat diet; NC, negative control; and RD, regular diet.

(as defined by nuclear translocation) of its downstream signaling mediator NFκB. These abnormalities were reduced by treatment with liraglutide (Figure 7A and B). Because activation of apoptosis has been demonstrated in the hearts of severely obese Zucker rats,[28] we examined whether this mechanism might account for the cardiac dysfunction observed in mice fed a HFD for 32 weeks. Despite appreciable increases in intramyocardial lipids, neither terminal deoxynucleotidyl transferase–mediated dUTP nick end-labeling nor Western blot analyses for activated caspase-3 detected any increase in apoptosis in hearts from 16- or 32-week mice fed HFD versus RD (Figure 7C through 7G). Of potential interest, levels of the microtubule-associated protein-1 light chain-3β, a marker of autophagy,[29] were also upregulated following treatment with liraglutide (online-only Data Supplement Figure II).

Liraglutide Corrected Obesity-Induced Cardiac Dysfunction Through an AMPK-Dependent Mechanism

Unlike the relatively silent cardiac phenotype after 16 weeks of HFD, heart weight was significantly increased in mice on HFD for 32weeks (150±5 versus RD, 136±4 mg, *P*<0.05, n=10/group), as was morphometry-defined cardiomyocyte size (12±0.8% greater surface area versus RD, *P*<0.01) with the observed fall in heart weight/BW ratio (3.2±0.1 versus 4.2±0.1 mg/g, *P*<0.0001) attributable to increased BW. Although baseline heart rates did not differ between HFD and RD groups (HFD, 612 ± 34 versus RD, 548 ± 16 beats/min, *P*=NS, n=10/group), and nor did they differ or change after 1 week of liraglutide (HFD, 573 ± 18, n=10 versus RD, 542±8, n=6, beats/min, *P*=NS for all comparisons), the load-dependent echocardiographic measure of fractional shortening was reduced in obese mice versus lean controls (30.3±0.7% versus 41.4±1.2%; *P*<0.05, n=10/group), with subsequent treatment with liraglutide for 1 week correcting this abnormality (preliraglutide, 30.3±0.7; after 1 week of liraglutide, 42.1±1.5%, *P*<0.05). Additional echocardiography data from the 32-week time point are provided in online-only Data Supplement Table III.

Because analysis of cardiac signaling pathways in obese mice had shown liraglutide-reversible inactivation (ie, dephosphorylation) of the energy sensor AMPK (Figure 4A), we next tested the role of AMPK in mediating the beneficial effects of liraglutide on cardiac function. Left ventricular performance was assessed in mice fed HFD or RD for 20 weeks, with obese animals receiving liraglutide or placebo for 1 week in the presence or absence of the AMPK inhibitor, compound C. Steady-state pressure-volume loops

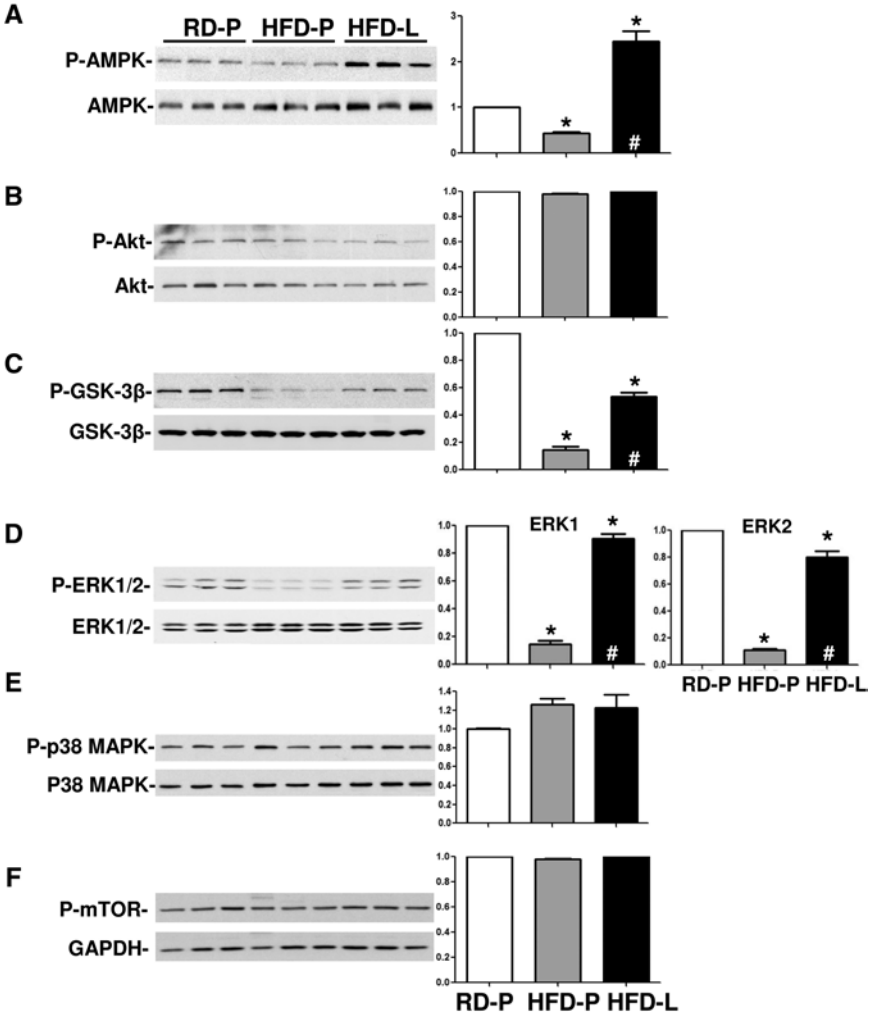

Figure 4. Treatment with a weight-neutral dose of a GLP-1 analog corrected the abnormalities in cardiac signaling caused by 32 weeks of HFD. Representative Western blots of left ventricular extracts from lean mice fed a RD and obese mice fed a HFD for 32 weeks are shown. Corresponding densitometric quantifications of the fold changes in phosphorylated/total protein relative to placebo-treated RD-fed animals are shown. Liraglutide treatment (L) for 1 week (30 μg/kg SC BID) increased phosphorylation of AMPK (**A**) but not Akt (**B**), and normalized phosphorylation of GSK3β (**C**) and ERK1/2 (**D**) in obese mice (HFD-L) in comparison with placebo-treated HFD-fed mice (HFD-P). Phosphorylation of p38-MAPK (**E**) and mTOR **(F)** did not change in response to HFD or drug treatment. Data shown are mean±SE; n=5 animals/group; 1-way ANOVA: **P*<0.05 versus RD-P, #*P*<0.05 versus HFD-P, by Tukey multiple comparison post hoc test. AMPK indicates AMP-activated protein kinase; ERK, extracellular-signal-regulated kinase; GLP-1, glucagon-like peptide-1; GSK-3β, glycogen synthase kinase 3β; HFD, high-fat diet; mTOR, mammalian target of rapamycin; p38 MAPK, p38 mitogen-activated protein kinase; and RD, regular diet.

revealed that obesity-induced increases in peak systolic pressure were reduced by liraglutide and that several measures of ventricular performance, including the load-independent isovolumic relaxation constant (τ) were also improved by treatment with liraglutide (Figure 8A through 8G). Importantly, these beneficial effects of the GLP-1 agonist were completely lost in the presence of compound C (Figure 8A through 8G). These data show that hearts of obese mice are functionally responsive to exogenous incretin therapy in an AMPK-dependent manner.

Liraglutide Normalized Markers of Cardiac Hypertrophy

Quantitative real-time polymerase chain reaction of left ventricular RNA (see online-only Data Supplement Table IV for primer sequences) showed that expression levels of established markers of cardiac hypertrophy, such as atrial natriuretic peptide, brain natriuretic peptide, and β-myosin heavy chain, and the β/α-myosin heavy chain ratio (RD, 0.4±0.1; HFD-P, 2.1±0.2; HFD-L, 0.5±0.1), as well, were increased in mice fed HFD for 20 weeks in comparison with age-matched RD-fed controls (Figure 8H). Importantly, treatment of obese mice with liraglutide returned these markers (and the β/α-myosin heavy chain ratio) to normal levels (Figure 8H; n=5/group, *P*<0.05).

Evidence for Direct Anti-inflammatory and Cytoprotective Effects of GLP-1R Activation

As treatment with liraglutide in vivo may exert cardiac effects via regulation of insulin, glucagon, or other physiological processes in other organ systems, we assessed the direct actions of liraglutide ex vivo. Both GLP-1 and liraglutide decreased the number of monocytes adhering to TNF-α–activated human umbilical vein endothelial cell cultures. Importantly, this effect could be blocked by the GLP-1R antagonist exendin (9–39) (online-only Data Supplement Figure III).

Obesity is also associated with elevated plasma free fatty acids that participate in the pathogenesis of insulin resistance.[30] As one of the most abundant saturated fatty acids in plasma, palmitate is markedly elevated following HFD,[31] and chronic exposure of rat neonatal cardiomyocytes to bovine serum albumin–bound palmitic acid (PA) produces a model of fatty acid–induced lipotoxicity in vitro.[32] Indeed, PA has also been used to induce cytopathology and myofibrillar degeneration in adult rat cardiomyocytes.[33] We investigated whether GLP-1R activation might prevent lipotoxicity in cardiomyocytes. This experiment revealed that the cell swelling and cytoskeletal disintegration caused by PA could be prevented by coincubation with liraglutide, the latter working through a GLP-1R–dependent mechanism (online-only Data Supplement Figure IVA). Moreover,

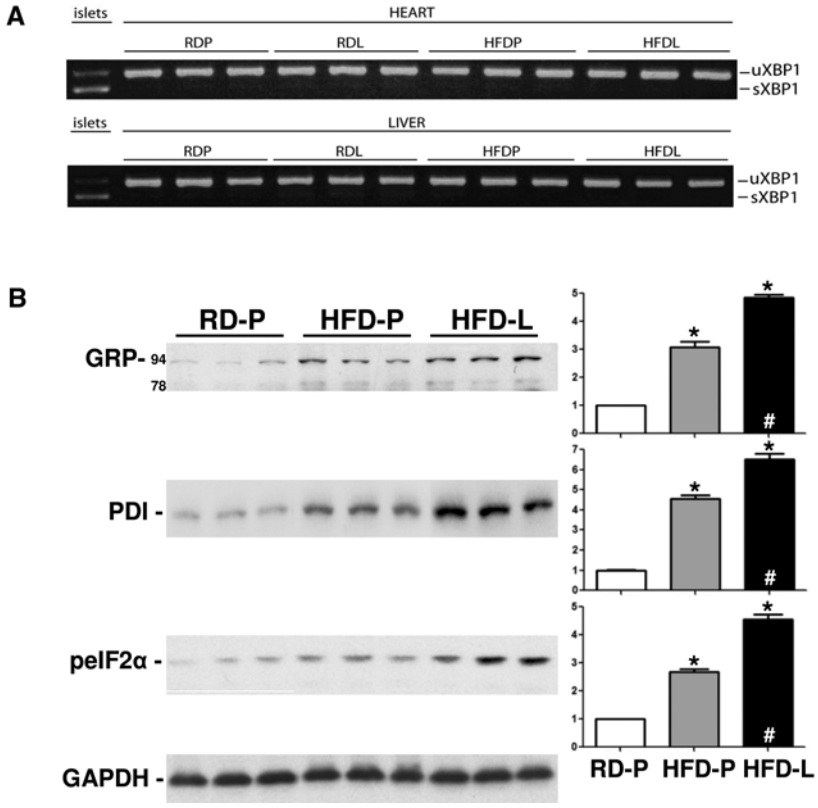

Figure 5. Treatment with a GLP-1 analog enhanced the increased cardiac expression of ER-related proteins caused by 32 weeks of HFD. **A**, Total RNA was isolated from ventricular tissue of mice fed either RD or HFD for 56 weeks and analyzed by RT-PCR and ethidium bromide–stained gel electrophoresis to detect unspliced (uXBP1) and spliced (sXBP1) forms of the ER-stress marker XBP1. Mouse islets treated with thapsigargin (Tg) served as a positive control. **B**, Representative Western blots and corresponding densitometric quantification of fold changes in GAPDH-normalized expression of ER-related markers, GRP, PDI, and peIF2α are shown for mice on RD or HFD for 32 weeks. Despite enhanced signal for ER-related proteins in hearts of HFD-P and HFD-L groups at 32 weeks, no splicing of XBP1 was observed in the hearts or livers of mice after even 56 weeks of HFD. Treatment with liraglutide enhanced cardiac expression levels of these ER-stress proteins in obese mice (HFD-L) in comparison with placebo (P). Data shown are mean±SE; n=5 animals/group; 1-way ANOVA: **P*<0.05 versus RD-P, #*P*<0.05 versus HFD-P by Tukey multiple comparison post hoc test. ANOVA indicates analysis of variance; ER, endoplasmic reticulum; GLP-1, glucagon-like peptide-1; GRP, glucose-regulated protein; HFD, high-fat diet; PDI, disulfide isomerase; peIF2α, eukaryotic translation initiation factor 2α; RD, regular diet; and RT-PCR, reverse transcription polymerase chain reaction.

under these harsh in vitro conditions, immunoblotting for activated caspase-3 revealed PA-induced apoptosis was also prevented by liraglutide (online-only Data Supplement Figure IVB).

Because obesity-associated increases in plasma free fatty acids also target other cardiovascular cell types, including vascular cells,[34] we conducted similar experiments in human coronary smooth muscle cells. Once again, liraglutide prevented PA-induced cell swelling and loss of cell viability (online-only Data Supplement Figure IVC and IVD).

Discussion

Obesity is a serious health problem. Excess caloric intake from fat can trigger obesity and contribute to dyslipidemia, insulin resistance, and type 2 diabetes mellitus, all of which are known risk factors for cardiovascular disease.[35] As observed in our study, HFD can directly affect the heart even before the onset of overt diabetes mellitus, although impaired glucose tolerance and insulin resistance are features of our model. The mechanisms involved include the induction of inflammation, hypertrophy, fibrosis, and contractile dysfunction.[2] As such, studies identifying therapies that prevent or reverse HFD-induced cardiac pathophysiology are of interest, because their translation to the clinic may impact both the incidence and severity of cardiovascular disease.

As regulators of glucose and lipid homeostasis,[12] potentiating endogenous GLP-1 by dipeptidyl peptidase-4 inhibitors or exogenous GLP-1 analogs show promise for the treatment of type 2 diabetes mellitus. Furthermore, direct benefits on the cardiovascular system may be a particular advantage of incretin-targeted therapies over other classes of antidiabetic drugs.[36] Underlying these effects are distinct and complementary mechanisms that include weight loss, improved glycemic control, enhanced insulin signaling, and direct effects on cardiovascular pathophysiology, including protection from ischemia-reperfusion injury and adverse cardiac remodeling following myocardial infarction.[20,22,37]

Here, we show that even brief (ie, 1 week) treatment with a weight-neutral dose of the GLP-1R agonist liraglutide can (a) ameliorate HFD-induced disturbances in glucose handling and insulin sensitivity, (b) reverse the expression

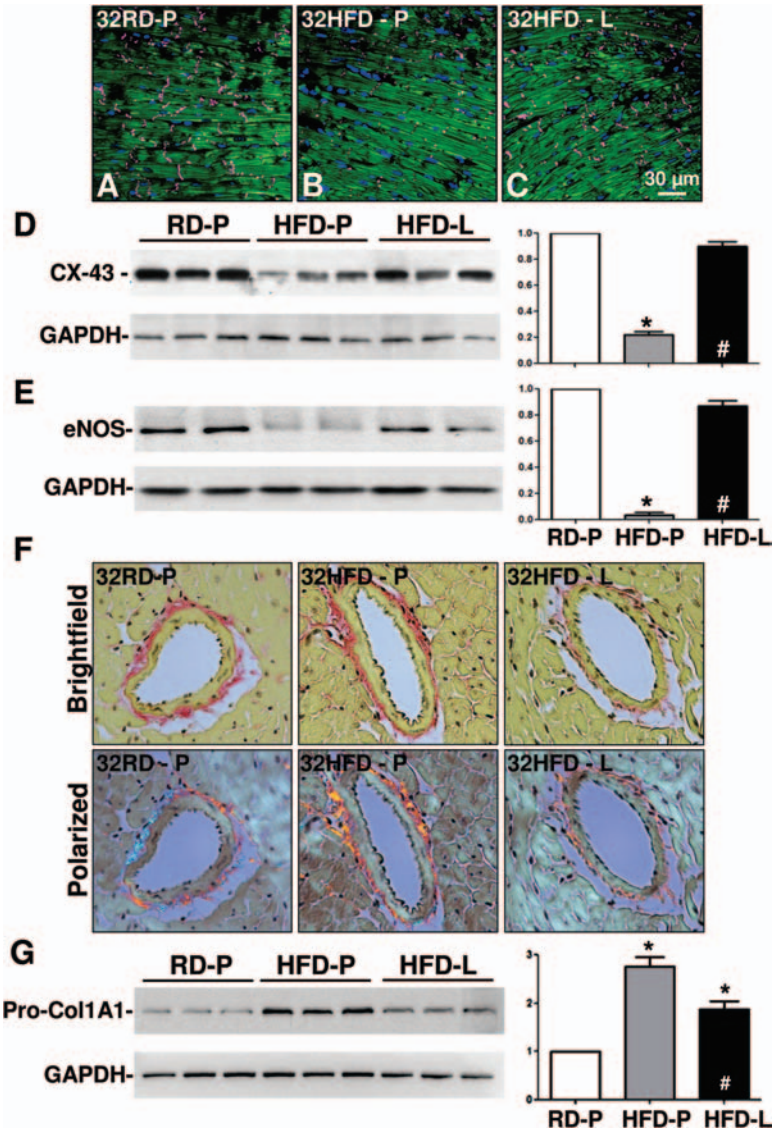

Figure 6. A GLP-1 analog corrected the abnormal cardiac expression levels of connexin 43, eNOS, and collagen caused by 32 weeks of HFD. In obese mice fed HFD for 32 weeks, confocal immunolabeling for the cardiac gap junction protein Cx-43 (pink) in sections costained for nuclei (DAPI, blue) and α-sarcomeric actinin (green) revealed reduced abundance of Cx-43 (**B**) in comparison with RD-fed controls (**A**). **C**, This abnormality was normalized by treating HFD-fed mice with liraglutide (L) for only 1 week. **D**, Western blot for total ventricular Cx-43 revealed the same result. **E**, HFD-induced obesity was also associated with decreased levels of cardiac eNOS, which was corrected by the GLP-1 analog. **F,** Picrosirius red-stained heart sections were imaged with brightfield and polarized light microscopy. Perivascular collagen under brightfield appears red. Thick collagen fibers under polarized light have yellow-orange birefringence, whereas thin collagen fibrils have green birefringence. HFD increased perivascular thick collagen deposition. Lean (RD-fed) mice retain predominantly fibrillar perivascular collagen. Treatment of HFD-fed mice with liraglutide reduced perivascular collagen staining, with reduced thick collagen fiber deposition. **G**, These histological findings were mirrored by Western blot for procollagen 1A1. Representative Western blots and corresponding densitometric quantification of fold changes in GAPDH-normalized expression of these proteins are shown. Data are mean±SE; n=5–6 animals/group; 1-way ANOVA: **P*<0.05 versus RD-P, #*P*<0.05 versus HFD-P, by Tukey multiple comparison post hoc test. Cx-43 indicates connexin-43; DAPI, 4′,6-diamidino-2-phenylindole; eNOS, endothelial nitric oxide synthase; GLP-1, glucagon-like peptide-1; HFD, high-fat diet; and RD, regular diet.

of inflammatory markers, (c) enhance ER-stress–related adaptive protein levels, (d) normalize key cardiac signaling pathways disrupted by HFD, (e) restore diminished levels of eNOS and Cx-43, and increased levels of procollagen 1A1, (f) normalize expression levels of hypertrophy markers, with (g) morphological evidence of reduced perivascular fibrosis, and (h) functional evidence of improved cardiac performance through an AMPK-dependent mechanism. To our knowledge, this study represents the first demonstration of perturbed cardiac Cx-43 expression in any model of obesity. Also novel are the results showing that liraglutide can correct this abnormality in gap junction protein expression and other obesity-associated decreases in eNOS and cardiac function in vivo without changes in BW. New data supporting direct GLP-1R–dependent effects on endothelial and cardiomyocyte biology include the ability of liraglutide to (i) inhibit adhesion of monocytes to TNF-α-activated endothelial cells, and (j) prevent lipotoxicity in cardiomyocytes and human coronary smooth muscle cells in vitro. By comparing the cardiac consequences of 16 versus 32 weeks of diet-induced obesity in the mouse, our study reveals that HFD-induced markers of inflammation (TNF-α, NFκB) and disturbed ER homeostasis (glucose-regulated protein 78, glucose-regulated protein 94, disulfide isomerase, phospho-eukaryotic translation initiation factor 2α) (at 16 weeks of HFD) are present before the onset of cardiac fibrosis, hypertrophy, and dysfunction (observed at 32 weeks of HFD). Although Ozcan et al[38] also showed increased expression of glucose-regulated protein and phospho-eukaryotic translation initiation factor 2α in livers of *ob/ob* mice and mice fed a HFD for 16 weeks, and also demonstrated increased insulin resistance in mice lacking the ER-stress transcription factor XBP1, no evidence for HFD-induced increases in XBP1 splicing was presented. In our study, we find no evidence for XBP1 splicing in the heart (or liver) after prolonged HFD, suggesting that HFD causes only mild ER stress, which induces an adaptive response (ie, increased chaperone capacity). We posit that liraglutide's remarkable ability to augment this response may enhance the capacity of the ER to protect the heart (and

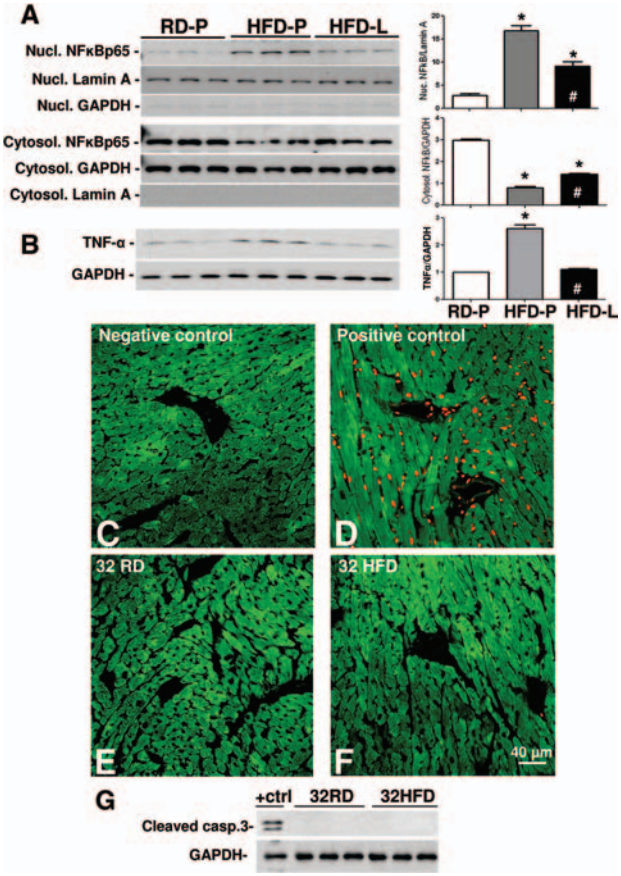

Figure 7. A GLP-1 analog reversed the expression of inflammatory markers in hearts of obese mice, which showed no evidence of apoptosis. Protein levels of activated NFκB-p65 (demonstrated by nuclear translocation) (**A**) and TNF-α (**B**) were increased in hearts of placebo (P)-treated mice fed HFD for 32 weeks (HFD-P) versus lean RD-fed controls (RD-P). Liraglutide treatment decreased inflammatory markers in HFD-fed mice (HFD-L). Data shown are mean±SE; n=4–6 animals/group; 1-way ANOVA: **P*<0.05 versus RD-P, #*P*<0.05 versus HFD-P, by Tukey multiple comparison post hoc test. Paraffin sections (6 μm) were stained for TUNEL to identify apoptotic nuclei (red). Negative (**C**, without terminal transferase) and positive (**D**, DNase I-treated) controls were included. Almost no TUNEL-positive nuclei are detectable in hearts from 32RD or 32HFD mice (**E, F**). Absence of apoptosis in these groups was confirmed by Western blot for cleaved caspase 3 (**G**), with thapsigargin-induced apoptosis in islet cells serving as a positive control (+ctrl). GLP-1 indicates glucagon-like peptide-1; HFD, high-fat diet; NFκB: NFκB, nuclear factor kappa B; RD, regular diet; TNF-α, tumor necrosis factor-α; and TUNEL, terminal deoxynucleotidyl transferase-mediated dUTP nick end-labeling.

human coronary smooth muscle cells) against lipotoxicity, as demonstrated in models of hepatocyte[19] and β-cell[39] lipotoxicity in vitro.

AMPK, Akt, GSK-3β, ERK1/2, and p38 mitogen-activated protein kinase are signaling molecules involved in the pathophysiology of a variety of cardiac diseases and models. Our studies reveal that HFD-induced obesity resulted in the dephosphorylation of some (ie, AMPK, GSK-3β, and ERK1/2), but not all (ie, p38 mitogen-activated protein kinase) of these molecular mediators in the mouse heart. Treatment with liraglutide effectively reversed abnormalities in each of the pathways affected by HFD-induced obesity. The effect of liraglutide on increased phosphorylation of the energy sensor AMPK is similar to that of the antidiabetic drug metformin, which also induced activation of this molecule in the hearts of obese mice.[40] Although our invasive hemodynamic studies suggested a key role for AMPK in the cardiovascular actions of liraglutide, further studies are needed to establish if more of the many pleiotropic benefits of liraglutide observed also depend on its ability to activate AMPK. Several lines of evidence support a central role for AMPK in obesity-induced heart disease. AMPKα1-knockout mice are more susceptible to HFD-induced obesity, inflammation, and insulin resistance,[41] and experience worse HFD-induced cardiac hypertrophy and contractile dysfunction.[42] In addition, upregulation of AMPK signaling improves myocardial perfusion in diabetic mice,[43] and activators of AMPK (eg, dexamethasone and metformin) promote survival in cardiomyocytes exposed to TNF-α, an effect abolished by an AMPK inhibitor.[44] Ko et al[4] showed that a HFD (55% fat by calories) for only 6 weeks reduced AMPK phosphorylation in cardiac tissue of C57BL/6 mice, a finding they associated with macrophage infiltration and cardiac inflammation. These authors suggested that cytokines interleukin 6 and TNF-α were involved in decreased AMPK activity and pathological modulation of cardiac glucose metabolism.[4]

With regard to the serine/threonine kinase GSK-3β, we demonstrate that it is dephosphorylated (ie, hyperactivated) in the hearts of obese mice. Because increased activity of total GSK-3 (ie, GSK-3α and β-isoforms) in skeletal muscle, liver, and adipose tissues has been associated with reduced insulin action in those tissues,[45] it is tempting to speculate that HFD-induced activation of GSK-3β may also play a role in obesity-induced heart disease. Again, short-term treatment with liraglutide resulted in an Akt-independent increase in phosphorylation (ie, inactivation) of GSK-3β, approaching levels seen in lean controls. Supporting the importance of this normalizing effect of liraglutide on GSK-3β are data suggesting that inactivating GSK-3β by the antioxidant metallothionein prevented the pathogenetic mechanisms of streptozotocin-induced diabetes mellitus in mice.[46]

Obesity is associated with a low-grade chronic inflammation characterized by infiltration of monocyte/macrophages in skeletal, cardiac, and adipose tissues,[4,47] and by abnormal production of proinflammatory cytokines including TNF-α.[7] Our results clearly indicate that treatment with a GLP-1 analog can reduce (a) expression of TNF-α and NFκB in the hearts of obese mice, and (b) adhesion of monocytes to TNF-α-activated endothelial cells in a GLP-1R–dependent manner. Importantly, the latter in vitro data were obtained in human cell lines, enhancing the potential translational significance of our findings.

In addition, reduced cardiac eNOS level in obese mice may be an indicator of coronary dysfunction, because eNOS-derived nitric oxide plays an important role in the regulation of coronary blood flow.[48] Therefore, restored cardiac eNOS in response to 1 week of treatment with liraglutide may have had a significant impact on cardiac

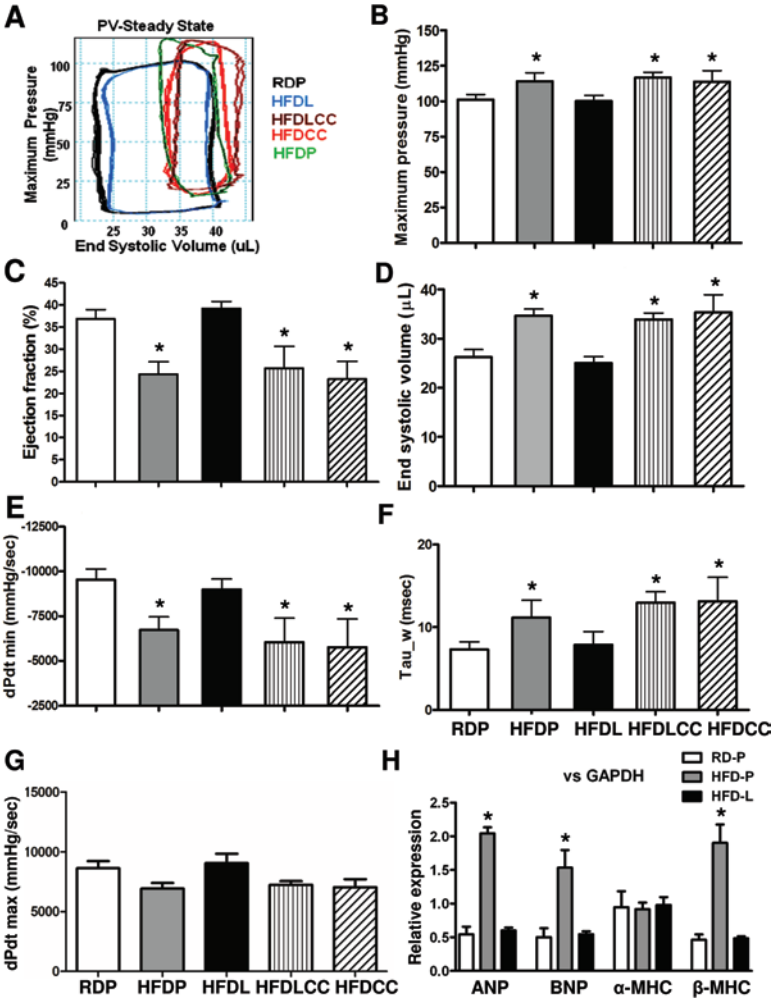

Figure 8. Liraglutide improved measures of cardiac performance through an AMPK-dependent mechanism. Invasive hemodynamic measurements were obtained in mice fed RD or HFD for 20 weeks. In the final week, some animals were treated with liraglutide (L) or placebo (P), in the presence of either the AMPK inhibitor compound C (CC) or its vehicle control. **A**, Representative steady-state PV loops from all groups are shown. **B**, Maximum left ventricular systolic pressure from all groups. **C** through **G**, Results of PV loop analyses showing measures of systolic (EF, ESV, dP/dtmax) and diastolic (dP/dtmin) function, including the load-independent isovolumic relaxation constant (Tau). One-way ANOVA: **P*<0.05 versus RD-P by Tukey multiple comparison post hoc test. **H**, Treatment with liraglutide also normalized the increased expression levels of ANP, BNP, and β-MHC observed in HFD-fed mice as determined by qRT-PCR. n=5–6⁄group; 1-way ANOVA: **P*<0.05 versus RD-P by Tukey multiple comparison post hoc test. AMPK indicates AMP-activated protein kinase; ANP, atrial natriuretic peptide; β-MHC, β-myosin heavy chain; BNP, brain natriuretic peptide; EF, ejection fraction; ESV, end-systolic volumes; HFD, high-fat diet; PV, pressure volume; qRT-PCR, quantitative reverse transcription polymerase chain reaction; and RD, regular diet.

function. With regard to Cx-43, it has been shown that cardiac inflammation can downregulate Cx-43 levels in the rat heart in a TNF-α–dependent manner.[49] Levels of Cx-43 are also reduced in the diabetic rat.[25] Because cardiac Cx-43 is required for coordinated electrical activity and is involved in the pathogenesis of cardiac arrhythmias,[50] repair of Cx-43 deficiency in the hearts of obese mice in our study may be another mechanism involved in the beneficial effects of the GLP-1 analog used.

Finally, exposure of mouse neonatal cardiomyocytes to PA resulted in cytopathological changes, including cellular swelling and cytoskeletal disintegration, which were blocked by cotreatment with liraglutide. That this effect could be abolished by a GLP-1R antagonist clearly supports a direct cardioprotective action of the agent.

In conclusion, the present study has shown, for the first time, how a short course of treatment with a weight-neutral dose of a GLP-1 analog can reverse the complex molecular pathophysiology of obesity-induced heart disease in mice through a variety of putative mechanisms, with a central role for AMPK (online-only Data Supplement Figure V). These data support further clinical exploration of a potential therapeutic role for GLP-1R agonists in obesity-induced cardiac disease.

Sources of Funding

This study was funded by operating grants to Drs Husain and Drucker from the Heart and Stroke Foundation of Ontario (HSFO; T6757 and NA6997) and by a grant to Dr Drucker from Novo Nordisk Inc. Dr Husain is recipient of a Career Investigator Award of the HSFO (CI6824). Dr Drucker received support from a Canada Research Chair in Regulatory Peptides and a Banting and Best Diabetes Center-Novo Nordisk Chair in Incretin Biology. Dr Billia is recipient of a Phase I Clinician-Scientist Award from the Canadian Institutes of Health Research (CIHR). Dr Volchuk is supported by an Operating Grant from the CIHR (MOP-114922) and a Canada Research Chair in Diabetes Research.

Disclosures

Drs Husain and Drucker have served as consultants for NovoNordisk, Merck & Co, and Hoffman La Roche with regard to their incretin-targeted therapeutics. They are recipients of investigator-initiated industry funding for distinct research projects from NovoNordisk and Merck & Co. The other authors report no conflicts.

References

1. Wisse BE, Kim F, Schwartz MW. Physiology. An integrative view of obesity. *Science*. 2007;318:928–929.
2. Abel ED, Litwin SE, Sweeney G. Cardiac remodeling in obesity. *Physiol Rev*. 2008;88:389–419.
3. Gregor MF, Hotamisligil GS. Inflammatory mechanisms in obesity. *Annu Rev Immunol*. 2011;29:415–445.

4. Ko HJ, Zhang Z, Jung DY, Jun JY, Ma Z, Jones KE, Chan SY, Kim JK. Nutrient stress activates inflammation and reduces glucose metabolism by suppressing AMP-activated protein kinase in the heart. *Diabetes*. 2009;58:2536–2546.
5. Hotamisligil GS. Endoplasmic reticulum stress and the inflammatory basis of metabolic disease. *Cell*. 2010;140:900–917.
6. Buettner R, Schölmerich J, Bollheimer LC. High-fat diets: modeling the metabolic disorders of human obesity in rodents. *Obesity (Silver Spring)*. 2007;15:798–808.
7. Hotamisligil GS, Shargill NS, Spiegelman BM. Adipose expression of tumor necrosis factor-alpha: direct role in obesity-linked insulin resistance. *Science*. 1993;259:87–91.
8. Uysal KT, Wiesbrock SM, Marino MW, Hotamisligil GS. Protection from obesity-induced insulin resistance in mice lacking TNF-alpha function. *Nature*. 1997;389:610–614.
9. Bahrami H, Bluemke DA, Kronmal R, Bertoni AG, Lloyd-Jones DM, Shahar E, Szklo M, Lima JA. Novel metabolic risk factors for incident heart failure and their relationship with obesity: the MESA (Multi-Ethnic Study of Atherosclerosis) study. *J Am Coll Cardiol*. 2008;51:1775–1783.
10. Ceylan-Isik AF, Sreejayan N, Ren J. Endoplasmic reticulum chaperon tauroursodeoxycholic acid alleviates obesity-induced myocardial contractile dysfunction. *J Mol Cell Cardiol*. 2011;50:107–116.
11. Hamid T, Guo SZ, Kingery JR, Xiang X, Dawn B, Prabhu SD. Cardiomyocyte NF-κB p65 promotes adverse remodelling, apoptosis, and endoplasmic reticulum stress in heart failure. *Cardiovasc Res*. 2011;89:129–138.
12. Drucker DJ. The biology of incretin hormones. *Cell Metab*. 2006;3:153–165.
13. Arakawa M, Mita T, Azuma K, Ebato C, Goto H, Nomiyama T, Fujitani Y, Hirose T, Kawamori R, Watada H. Inhibition of monocyte adhesion to endothelial cells and attenuation of atherosclerotic lesion by a glucagon-like peptide-1 receptor agonist, exendin-4. *Diabetes*. 2010;59:1030–1037.
14. McClean PL, Parthsarathy V, Faivre E, Hölscher C. The diabetes drug liraglutide prevents degenerative processes in a mouse model of Alzheimer's disease. *J Neurosci*. 2011;31:6587–6594.
15. Yusta B, Baggio LL, Estall JL, Koehler JA, Holland DP, Li H, Pipeleers D, Ling Z, Drucker DJ. GLP-1 receptor activation improves beta cell function and survival following induction of endoplasmic reticulum stress. *Cell Metab*. 2006;4:391–406.
16. Field BC, Chaudhri OB, Bloom SR. Obesity treatment: novel peripheral targets. *Br J Clin Pharmacol*. 2009;68:830–843.
17. Novo-Nordisk. Effect of liraglutide on body weight in non-diabetic obese subjects or overweight subjects with co-morbidities: a randomised, double-blind, placebo controlled, parallel group, multi-centre, multinational trial with stratification of subject to either 56 or 160 weeks of treatment based on pre-diabetes status at randomisation. Phase iii clinical trial.Scale™ - obesity and pre-diabetes. http://www.Clinicaltrials.Gov/ct2/show/nct01272219. Accessed August 31, 2012.
18. Mells JE, Fu PP, Sharma S, Olson D, Cheng L, Handy JA, Saxena NK, Sorescu D, Anania FA. Glp-1 analog, liraglutide, ameliorates hepatic steatosis and cardiac hypertrophy in C57BL/6J mice fed a Western diet. *Am J Physiol Gastrointest Liver Physiol*. 2012;302:G225–G235.
19. Sharma S, Mells JE, Fu PP, Saxena NK, Anania FA. GLP-1 analogs reduce hepatocyte steatosis and improve survival by enhancing the unfolded protein response and promoting macroautophagy. *PLoS ONE*. 2011;6:e25269.
20. Ban K, Noyan-Ashraf MH, Hoefer J, Bolz SS, Drucker DJ, Husain M. Cardioprotective and vasodilatory actions of glucagon-like peptide 1 receptor are mediated through both glucagon-like peptide 1 receptor-dependent and -independent pathways. *Circulation*. 2008;117:2340–2350.
21. Ban K, Kim KH, Cho CK, Sauvé M, Diamandis EP, Backx PH, Drucker DJ, Husain M. Glucagon-like peptide (GLP)-1(9-36)amide-mediated cytoprotection is blocked by exendin(9-39) yet does not require the known GLP-1 receptor. *Endocrinology*. 2010;151:1520–1531.
22. Noyan-Ashraf MH, Momen MA, Ban K, Sadi AM, Zhou YQ, Riazi AM, Baggio LL, Henkelman RM, Husain M, Drucker DJ. GLP-1R agonist liraglutide activates cytoprotective pathways and improves outcomes after experimental myocardial infarction in mice. *Diabetes*. 2009;58:975–983.
23. Sachdeva MM, Claiborn KC, Khoo C, Yang J, Groff DN, Mirmira RG, Stoffers DA. Pdx1 (MODY4) regulates pancreatic beta cell susceptibility to ER stress. *Proc Natl Acad Sci USA*. 2009;106:19090–19095.
24. Asbun J, Villarreal FJ. The pathogenesis of myocardial fibrosis in the setting of diabetic cardiomyopathy. *J Am Coll Cardiol*. 2006;47:693–700.
25. Lin H, Ogawa K, Imanaga I, Tribulova N. Remodeling of connexin 43 in the diabetic rat heart. *Mol Cell Biochem*. 2006;290:69–78.
26. Mueller EE, Momen A, Massé S, Zhou YQ, Liu J, Backx PH, Henkelman RM, Nanthakumar K, Stewart DJ, Husain M. Electrical remodelling precedes heart failure in an endothelin-1-induced model of cardiomyopathy. *Cardiovasc Res*. 2011;89:623–633.
27. Valerio A, Cardile A, Cozzi V, Bracale R, Tedesco L, Pisconti A, Palomba L, Cantoni O, Clementi E, Moncada S, Carruba MO, Nisoli E. TNF-alpha downregulates eNOS expression and mitochondrial biogenesis in fat and muscle of obese rodents. *J Clin Invest*. 2006;116:2791–2798.
28. Lee SD, Tzang BS, Kuo WW, Lin YM, Yang AL, Chen SH, Tsai FJ, Wu FL, Lu MC, Huang CY. Cardiac fas receptor-dependent apoptotic pathway in obese Zucker rats. *Obesity (Silver Spring)*. 2007;15:2407–2415.
29. Barth S, Glick D, Macleod KF. Autophagy: assays and artifacts. *J Pathol*. 2010;221:117–124.
30. Oprescu AI, Bikopoulos G, Naassan A, Allister EM, Tang C, Park E, Uchino H, Lewis GF, Fantus IG, Rozakis-Adcock M, Wheeler MB, Giacca A. Free fatty acid-induced reduction in glucose-stimulated insulin secretion: evidence for a role of oxidative stress in vitro and in vivo. *Diabetes*. 2007;56:2927–2937.
31. Boden G. Interaction between free fatty acids and glucose metabolism. *Curr Opin Clin Nutr Metab Care*. 2002;5:545–549.
32. Sparagna GC, Hickson-Bick DL, Buja LM, McMillin JB. Fatty acid-induced apoptosis in neonatal cardiomyocytes: redox signaling. *Antioxid Redox Signal*. 2001;3:71–79.
33. Dyntar D, Eppenberger-Eberhardt M, Maedler K, Pruschy M, Eppenberger HM, Spinas GA, Donath MY. Glucose and palmitic acid induce degeneration of myofibrils and modulate apoptosis in rat adult cardiomyocytes. *Diabetes*. 2001;50:2105–2113.
34. Staiger H, Staiger K, Stefan N, Wahl HG, Machicao F, Kellerer M, Häring HU. Palmitate-induced interleukin-6 expression in human coronary artery endothelial cells. *Diabetes*. 2004;53:3209–3216.
35. Chess DJ, Stanley WC. Role of diet and fuel overabundance in the development and progression of heart failure. *Cardiovasc Res*. 2008;79:269–278.
36. Mundil D, Noyan-Ashraf MH, Husain M. The incretin system and cardiovascular risk: Effects of incretin-targeted therapies. *Curr Cardiovasc Risk Rep*. 2011;5:62–69.
37. Sauvé M, Ban K, Momen MA, Zhou YQ, Henkelman RM, Husain M, Drucker DJ. Genetic deletion or pharmacological inhibition of dipeptidyl peptidase-4 improves cardiovascular outcomes after myocardial infarction in mice. *Diabetes*. 2010;59:1063–1073.
38. Ozcan U, Cao Q, Yilmaz E, Lee AH, Iwakoshi NN, Ozdelen E, Tuncman G, Görgün C, Glimcher LH, Hotamisligil GS. Endoplasmic reticulum stress links obesity, insulin action, and type 2 diabetes. *Science*. 2004;306:457–461.
39. Cunha DA, Ladrière L, Ortis F, Igoillo-Esteve M, Gurzov EN, Lupi R, Marchetti P, Eizirik DL, Cnop M. Glucagon-like peptide-1 agonists protect pancreatic beta-cells from lipotoxic endoplasmic reticulum stress through upregulation of BiP and JunB. *Diabetes*. 2009;58:2851–2862.
40. Gundewar S, Calvert JW, Jha S, Toedt-Pingel I, Ji SY, Nunez D, Ramachandran A, Anaya-Cisneros M, Tian R, Lefer DJ. Activation of AMP-activated protein kinase by metformin improves left ventricular function and survival in heart failure. *Circ Res*. 2009;104:403–411.
41. Zhang W, Zhang X, Wang H, Guo X, Li H, Wang Y, Xu X, Tan L, Mashek MT, Zhang C, Chen Y, Mashek DG, Foretz M, Zhu C, Zhou H, Liu X, Viollet B, Wu C, Huo Y. AMP-activated protein kinase α1 protects against diet-induced insulin resistance and obesity. *Diabetes.* July 24, 2012. doi: 10.2337/db11-1373. http://diabetes.diabetesjournals.org. Accessed November 5, 2012.
42. Turdi S, Kandadi MR, Zhao J, Huff AF, Du M, Ren J. Deficiency in AMP-activated protein kinase exaggerates high fat diet-induced cardiac hypertrophy and contractile dysfunction. *J Mol Cell Cardiol*. 2011;50:712–722.
43. Kusmic C, L'abbate A, Sambuceti G, Drummond G, Barsanti C, Matteucci M, Cao J, Piccolomini F, Cheng J, Abraham NG. Improved myocardial perfusion in chronic diabetic mice by the up-regulation of pLKB1 and AMPK signaling. *J Cell Biochem*. 2010;109:1033–1044.

44. Kewalramani G, Puthanveetil P, Wang F, Kim MS, Deppe S, Abrahani A, Luciani DS, Johnson JD, Rodrigues B. AMP-activated protein kinase confers protection against TNF-{alpha}-induced cardiac cell death. *Cardiovasc Res*. 2009;84:42–53.
45. Henriksen EJ. Dysregulation of glycogen synthase kinase-3 in skeletal muscle and the etiology of insulin resistance and type 2 diabetes. *Curr Diabetes Rev*. 2010;6:285–293.
46. Wang Y, Feng W, Xue W, Tan Y, Hein DW, Li XK, Cai L. Inactivation of GSK-3beta by metallothionein prevents diabetes-related changes in cardiac energy metabolism, inflammation, nitrosative damage, and remodeling. *Diabetes*. 2009;58:1391–1402.
47. Wellen KE, Hotamisligil GS. Inflammation, stress, and diabetes. *J Clin Invest*. 2005;115:1111–1119.
48. Gödecke A, Decking UK, Ding Z, Hirchenhain J, Bidmon HJ, Gödecke S, Schrader J. Coronary hemodynamics in endothelial NO synthase knockout mice. *Circ Res*. 1998;82:186–194.
49. Fernandez-Cobo M, Gingalewski C, Drujan D, De Maio A. Downregulation of connexin 43 gene expression in rat heart during inflammation. The role of tumour necrosis factor. *Cytokine*. 1999;11:216–224.
50. Lerner DL, Yamada KA, Schuessler RB, Saffitz JE. Accelerated onset and increased incidence of ventricular arrhythmias induced by ischemia in Cx43-deficient mice. *Circulation*. 2000;101:547–552.

CLINICAL PERSPECTIVE

This study reveals the heretofore unrecognized ability of a glucagon-like peptide-1 analog to reverse multiple molecular mechanisms underlying the pathophysiology of obesity-induced cardiovascular dysfunction. Although this class of antidiabetic drug is under Food and Drug Administration–mandated evaluation for long-term cardiovascular safety, it will be many years before these data are reported. Meanwhile, this drug class is also being tested for its ability to reduce body weight, with a very limited understanding of how it affects the vulnerable cardiovascular systems of obese subjects. In this context, the findings of direct cardiovascular benefit of liraglutide in an animal model of obesity in vivo and cell culture models of inflammatory cell adhesion and lipotoxicity in vitro have promising implications for the clinical use of these agents in obesity.

SUPPLEMENTAL MATERIAL

Noyan-Ashraf *et al*.

A glucagon-like peptide-1 analogue reverses the molecular pathology and cardiac dysfunction of a mouse model of obesity

MS ID# CIRCULATIONAHA/2012/091215

SUPPLEMENTAL METHODS

Morphometry and immunohistochemistry: Paraffin-embedded hearts (N=6/group) were sectioned (6 μm) and stained with Masson's trichrome. Cardiomyocyte cross-sectional areas and fibrosis were quantified by Image-J (NIH) and Imagescope (Aperio) software. Collagen accumulation was assessed by picrosirius red-staining of sections from the mid-ventricle of each heart (N=4 per group, 4 sections per animal) imaged under brightfield and polarized light. Paraffin sections (5 μm) were also processed for heat-induced antigen retrieval in citrate buffer (pH=6), and co-immunolabelled overnight with rabbit polyclonal anti-connexin 43 and goat polyclonal anti-cardiac troponin I antibodies (Abs). For neutral lipid staining, 4% paraformaldehyde-fixed hearts (N=3/group) were cryoembedded and frozen sections (6 μm) were stained with oil-red-O and counterstained with hematoxylin. For assessment of intracellular ceramide, sections were stained with an anti-ceramide Ab. Liver from HFD-fed mice with significant steatosis served as positive control. Insulin-induced GLUT4 membrane translocation was visualized with confocal microscopy of frozen sections (4 μm) from 4% paraformaldehyde-fixed hearts (N=3/group) harvested 15 min after i.p. injection of insulin (2 IU/kg) or PBS-control (as detailed for insulin sensitivity test below) and stained with a goat polyclonal anti-GLUT4 antibody. Sections were incubated with fluorescent-tagged secondary Abs and Hoechst nuclear staining before mounting and imaging on a FluoView 1000 Laser Scanning Confocal Microscope (Olympus). For quantification of cardiac ceramide, z-stacks (0.1 μm steps) were acquired from ceramide signals and integrated density was measured by defining regions of interest (ROIs) in four high magnification areas per section. Four mid-ventricular cross-sections for each heart at 100 μm intervals were analyzed using Fluoview software version 3.1. Data were expressed as number of pixels per μm^2 (integrated density/area). See ***Supplemental Table 1*** for all Ab details.

Western blot: For assessment of signaling pathways, GLUT4, eNOS, connexin 43, atrial natriuretic peptide (ANP), ER-stress, and selected mitochondrial, inflammation, apoptosis and autophagy markers, protein extracts from the left ventricle of 16- and 32-week HFD- and RD-fed mice were run on denaturing gels, blotted and hybridized with 1^o Abs overnight. For NFκB, nuclear and cytosolic extracts were prepared as previously described[1]. HRP-conjugated 2^o Abs were visualized with chemiluminescence. See ***Supplemental Table 1*** for antibody details.

TUNEL assay: Cardiomyocyte apoptosis was quantified with the In Situ Cell Death Detection Kit (TMR red, Roche, Cat# 12 156 792 910) was used as per the manufacturer's instructions..

Cell adhesion: The human monocyte cell line THP1 was cultured in RPMI-1640 (Sigma) with 5% FBS. Primary human umbilical vein endothelial cells (HUVEC) were cultured in EBM-2 medium with Clonetics® EGM-2 SingleQuots® (Lonza). Only cells below passage 10 were used. HUVECs were seeded (~1x104/well) into clear bottom 96-well plates, grown to confluence and serum starved for 18-24 h. The wells were aspirated and replenished with EBM-2 medium alone or with TNF-α (20 ng/mL) for 4 h. HUVECs were then incubated with PBS in the presence or absence of the GLP-1R antagonist exendin(9-39) (10 μM) for 20 mins, then washed and incubated with PBS in the presence of GLP-1 (10-100 nM) or liragutide (100 nM) for 1 h. THP-1 cells were labelled with calcein-AM for 30 min, washed once in PBS, pelleted (1,500 rpm x 5 min) and resuspended in serum-free RPMI-1640 (1x106 cells/mL). THP-1 cells were then

allowed to settle on the HUVEC monolayer ($1x10^5$ cells/well) for 30 min. Plates were centrifuged (100g x 1 min) upside down to remove non-adherent cells. A plate reader was used to measure the fluorescence intensity of each well (494-517nm for calcein-AM). Fluorescence intensities were normalized to the un-stimulated condition (i.e. absent TNFα). Data shown represent means ± SEM from at least 3 independent experiments.

Lipotoxicity: Serum-deprived neonatal cardiomyocytes from C57BL/6 mice[2] were exposed to vehicle, palmitic acid (250 μM)[3], or the latter plus liraglutide (100 nM), or liraglutide and exendin(9-39) for 18 h in triplicates before harvest and confocal microscopy. Primary human coronary artery smooth muscle cells (HCSMC) were purchased from Cascade Biologicals (Gibco, C-017-5C) and maintained in M321 media (Gibco, M-231) supplemented with smooth muscle growth supplement and 1% pennicilin/streptomycin (Gibco, 15140). HCSMC were grown to 70% confluence. Prior to treatment, growth media was changed to supplement-free media for 24 h. Cells were treated with vehicle or palmitic acid (250 μM) with and without liraglutide (100 nM) liraglutide for 24 h. Whole cell lysates were collected for assessment of cell viability[4]as per the manufacturer's protocol (XTT assay, Roche). Each condition was done in triplicate, and the experiment performed three times. Phase contrast micrographs were also taken from HCSMC at the end of the incubation period for morphological assessment.

Metabolic testing: Intraperitoneal glucose tolerance test (IPGTT) and *in vivo* insulin sensitivity assessments were performed following a 6 h fast in placebo and liraglutide-treated 16HFD and age-matched 16RD controls (N=4/group). For IPGTT, D-glucose (Sigma, G5767-700G, 1 g/kg) was injected i.p. at time 0, and tail vein blood glucose levels were measured at -30, 0, 30, 60, 90 and 120 min from i.p. glucose administration with a Bayer Contour glucometer. In different animals, insulin sensitivity was examined at 10 min following an i.p. injection of insulin (2 IU /kg of Novolin GE, Novo Nordisk) or an equal volume of PBS (control). After cervical dislocation liver and heart tissue samples were isolated, and snap-frozen in liquid N2. Protein extracts were immunoblotted for well-known downstream signals of insulin action, such as phosphorylated IRS1, and phosphorylated and total Akt, GSK3β and ERK1/2. GAPDH was used as a loading control for IRS1.

Blood glucose: Blood glucose level was measured through a tail nick using a handheld glucometer and One-Touch strips (LifeScan) following overnight fast.

Plasma cholesterol and triglyceride levels: Blood collected by saphenous vein puncture of 16HFD and 16RD animals (N = 14/group) was centrifuged for 10 min at 10,000 g to obtain plasma. Cholesterol and triglyceride levels were determined by standardized assays performed at the core biochemistry laboratory of the Toronto Center for Phenogenomics (TCP).

XBP1 splicing assay: Total RNA extracted from heart and liver of mice on HFD for 32- and 56-weeks were examined for expression levels of spliced and unspliced XBP-1 by RT-PCR (Qiagen OneStep) using primers flanking the intron excised by IRE1 exonuclease activity. Primer sequences used were 5'-GAA-CCA-GGA-GTT-AAG-AAC-ACG-3' and 5'-AGG-CAACAG-TGT-CAG-AGT-CC-3'. PCR conditions were: 50 °C (30 min); 95 °C (15 min); 30 cycles of 94 °C (1 min), 55 °C (1 min), 72 °C (1min); 72 °C (10 min). RT-PCR products were resolved on a

3% agarose gel and visualized using ethidium bromide. Total RNA isolated from mouse islets treated with thapsigargin (Tg,1 μM, 1h) served as positive control for XBP-1 splicing.

Cardiac hypertrophy: Heart-to-body weight ratios were calculated for each animal at the time of sacrifice. To complement measurements of cardiomyocyte cross-sectional area (see above), quantitative real time-PCR for hypertrophy markers (α-MHC, β-MHC, ANP and BNP)[5] and the housekeeping gene GAPDH was performed on total RNA isolated from LV of placebo- and liraglutide-treated mice fed HFD for 20 weeks or RD-fed controls. See ***Supplemental Table 4*** for primer sequences.

Cardiac hemodynamics: To investigate hemodynamic effects of liraglutide, and its potential dependence on AMPK signaling, LV pressure-volume loops were obtained on mice fed HFD for 20 weeks and treated for 1 week with liraglutide, the AMPK inhibitor Compound C (P-5449, Sigma Aldrich; 10 mg/kg i.p, every other day[6, 7]) or vehicle. Under 1% isoflurane, a 1.4F micro manometer and conductance catheter (SPR-839) was introduced into the LV through the apex. LV pressures and volumes, ejection fraction, dP/dt, and the isovolumic relaxation time constant (Tau), a load-independent index of diastolic function, were computed using the PVAN software (Millar Instruments). Volume calibration of the system was performed to convert relative volume units to actual volumes[8].

Echocardiography: Mice on HFD for 32 weeks and age-matched lean RD-fed controls (N=6/group) underwent M-mode echocardiography before and after 7 days of liraglutide or placebo by an expert operator blinded to treatment assignment as previously described[9]. In this manner, each animal served as its own control.

REFERENCES FOR SUPPLEMENTAL METHODS

1. Battiprolu PK, Hojayev B, Jiang N, Wang ZV, Luo X, Iglewski M, Shelton JM, Gerard RD, Rothermel BA, Gillette TG, Lavandero S, Hill JA. Metabolic stress-induced activation of foxo1 triggers diabetic cardiomyopathy in mice. *J Clin Invest*. 2012;122:1109-1118
2. Noyan-Ashraf MH, Momen MA, Ban K, Sadi AM, Zhou YQ, Riazi AM, Baggio LL, Henkelman RM, Husain M, Drucker DJ. Glp-1r agonist liraglutide activates cytoprotective pathways and improves outcomes after experimental myocardial infarction in mice. *Diabetes*. 2009;58:975-983
3. Karaskov E, Scott C, Zhang L, Teodoro T, Ravazzola M, Volchuk A. Chronic palmitate but not oleate exposure induces endoplasmic reticulum stress, which may contribute to ins-1 pancreatic beta-cell apoptosis. *Endocrinology*. 2006;147:3398-3407
4. Hui S, Choi J, Zaidi S, Momen A, Steinbach SK, Sadi AM, Ban K, Husain M. Peptide-mediated disruption of calmodulin-cyclin e interactions inhibits proliferation of vascular smooth muscle cells and neointima formation. *Circ Res*. 2011;108:1053-1062
5. Caron KM, James LR, Kim HS, Knowles J, Uhlir R, Mao L, Hagaman JR, Cascio W, Rockman H, Smithies O. Cardiac hypertrophy and sudden death in mice with a genetically clamped renin transgene. *Proc Natl Acad Sci U S A*. 2004;101:3106-3111

6. Kim EK, Miller I, Aja S, Landree LE, Pinn M, McFadden J, Kuhajda FP, Moran TH, Ronnett GV. C75, a fatty acid synthase inhibitor, reduces food intake via hypothalamic amp-activated protein kinase. *J Biol Chem*. 2004;279:19970-19976
7. Kondo M, Shibata R, Miura R, Shimano M, Kondo K, Li P, Ohashi T, Kihara S, Maeda N, Walsh K, Ouchi N, Murohara T. Caloric restriction stimulates revascularization in response to ischemia via adiponectin-mediated activation of endothelial nitric-oxide synthase. *J Biol Chem*. 2009;284:1718-1724
8. Fazel S, Cimini M, Chen L, Li S, Angoulvant D, Fedak P, Verma S, Weisel RD, Keating A, Li RK. Cardioprotective c-kit+ cells are from the bone marrow and regulate the myocardial balance of angiogenic cytokines. *J Clin Invest*. 2006;116:1865-1877
9. Hoefer J, Azam MA, Kroetsch JT, Leong-Poi H, Momen MA, Voigtlaender-Bolz J, Scherer EQ, Meissner A, Bolz SS, Husain M. Sphingosine-1-phosphate-dependent activation of p38 mapk maintains elevated peripheral resistance in heart failure through increased myogenic vasoconstriction. *Circ Res*. 2010;107:923-933

Supplemental Table 1: Primary & secondary antibodies employed.

Primary antibodies (Cat #)	Source	Supplier	Dilution	Application(s)
Alpha-Actinin	Mo MC	Sigma	1:500	IF
Akt (9272)	Rab PC	Cell Signaling Technol.	1:1000	WB
P-Akt (9271) (Ser473)	Rab PC	Cell Signaling Technol.	1:1000	WB
AMPK (2603)	Rab MC	Cell Signaling Technol.	1:1000	WB
P-AMPKα (2535) (Thr172)	Rab MC	Cell Signaling Technol.	1:1000	WB
ANP (sc-18811)	Goat PC	Santa Cruz Biotechnol.	1:500	WB
Ceramide (MID 15B4)	Mo MC	Enzo Life Sciences	1:400	IF
Cx43 (3512)	Rab PC	Cell Signaling Technol.	1:100 & 1:1000	IF &WB
Pro-Col.1A1 (sc-30136)	Rab PC	Santa Cruz Biotechnol.	1:500	WB
Cleaved Caspase 3(Asp175) (9661)	Rab PC	Cell Signaling Technol	1:500	WB
COX IV (4844)	Rab PC	Cell Signaling Technol.	1:5000	WB
Cytochrome C (sc-7159)	Rab PC	Santa Cruz Biotechnol.	1:200 &1:2000	IF & WB
eNOS (9672)	Rab PC	Cell Signaling Technol.	1:1000	WB
P-eIF2α (9721) (Ser 51)	Rab PC	Cell Signaling Technol.	1:500	WB
ERK ½ (4695)	Rab MC	Cell Signaling Technol.	1:1000	WB
P-ERK ½ (9101) (Thr 202/Tyr 204)	Rab PC	Cell Signaling Technol.	1:1000	WB
GAPDH (sc-25778)	Rab PC	Santa Cruz Biotechnol.	1:10000	WB
Glut4 (sc-1608)	Goat PC	Santa Cruz Biotechnol.	1:100, 1:500	IF, WB
GSK3β (9315)	Rab PC	Cell Signaling Technol.	1:1000	WB
P-GSK3β (9336) (Ser 9)	Rab PC	Cell Signaling Technol.	1:1000	WB
P-IRS1(07-247) (Ser307)	Rab PC	Upstate	1:1000	WB
KDEL (GRP78/94) (SPA-827)	Mo MC	Stressgen	1:2000	WB
Lamin A (H-102) (sc-20680)-	Rab PC	Santa Cruz Biotechnol.	1:1000	WB
LC3A/B (4108)	Rab PC	Cell Signaling Technol.	1: 4000	WB
P-mTOR (2971)	Rab PC	Cell Signaling Technol.	1: 1000	WB
NFkBp65 (sc-372)	Rab PC	Santa Cruz Biotechnol.	1:2000	WB
PDI (SPA-890)	Rab PC	Stressgen	1:2000	WB
PGC-1α (sc-13067)	Rab PC	Santa Cruz Biotechnol.	1:2000	WB
TNFα (sc-1351)	Goat PC	Santa Cruz Biotechnol.	1:500	WB
Troponin I-C (sc-31655)	Goat PC	Santa Cruz Biotechnol.	1:200	IF
Troponin T, Cardiac isoform (MS-295-P0)	Mo MC	Thermo Scientific	1:400	IF
p38MAPK (9212)	Rab PC	Cell Signaling Technol.	1:1000	WB
P-p38MAPK (9211) (Thr 180/Tyr 182)	Rab PC	Cell Signaling Technol.	1:1000	WB
Secondary antibodies (Cat #)	**Source**	**Supplier**	**Dilution**	**Application(s)**
Anti-Mouse IgG-HRP conjugate (170-6516)	Goat	BioRad	1:10000	WB
Anti-Goat IgG-HRP conjugate (sc-2384)	Bovine	Santa Cruz Biotechnol.	1:5000	WB
Anti-Rab IgG-HRP conjugate (170-6515)	Goat	BioRad	1:10000	WB
Anti-Mouse AlexaFluor 647 (A10042)	Donkey	Invitrogen	1:400	IF
Anti-Goat AlexaFluor 488 (A-11055)	Donkey	Invitrogen	1:400	IF
Anti-Rabbit AlexaFluor 568 (A-10042)	Donkey	Invitrogen	1:400	IF

The name, supplier and dilutions of all Abs used for Western blot (WB) and immunofluorescence (IF) microscopy are provided. MC, monoclonal; PC, polyclonal; Mo, mouse; Rab, rabbit.

Supplemental Table 2: Body weights and fasting blood glucose determinations.

Group	Initial BW (g)	BW pre-treatment (g)	BW post-treatment (g)	FBG pre-treatment (mmol/L)	FBG post-treatment (mmol/L)
16 RD-P (N=10)	24.78 ± 0.44	31.80 ± 1.33*	30.87 ± 1.01	7.88 ± 0.38	7.55 ± 0.41
16 RD-L (N=10)	24.38 ± 0.38	29.5 ± 0.69*	28.92 ± 0.73	7.57 ± 0.27	7.00 ± 0.25**
16 HFD-P (N=10)	24.73 ± 0.94	44.18 ± 1.87*	43.62 ± 1.57	8.95 ± 0.38	8.86 ± 0.48
16 HFD-L (N=10)	25.68 ± 0.58	45.7 ± 1.27*	44.05 ± 0.54	8.31 ± 0.26	6.73 ± 0.26**
20RD (N=6)	22.8 ± 0.7	30.85 ± 0.4*	30.9 ± 0.7	ND	ND
20HFD-P (N=6)	21.7 ± 0.4	49.8 ± 0.6*	48.4 ± 0.9	ND	ND
20HFD-L (N=6)	20.6 ± 0.7	47.3 ± 1.0*	45.8 ± 1.1	ND	ND
32 RD-P (N=10)	23.6 ± 0.27	33.46 ± 1.5*	32.25 ± 1.56	8.88 ± 0.38	7.55 ± 0.41
32 RD-L (N=10)	24.35 ± 0.7	33.77 ± 0.64*	32.71 ± 0.45	9.64 ± 0.49	7.57 ± 0.27**
32 HFD-P (N=10)	25.3 ± 0.7	54.25 ± 0.62*	52.25 ± 0.1	8.4 ± 0.29	11.35 ± 0.38**
32 HFD-L (N=10)	26.82 ± 1.32	51.78 ± 1.16*	49.36 ± 0.48	9.02 ± 0.5	6.72 ± 0.27**
56 RD-P (N=3)	24.43 ± 0.63	36.22 ± 1.9*	35.68 ± 1.8	8.93 ± 0.13	9.1 ± 0.32
56 RD-L (n=3)	23.83 ± 1.37	35.26 ± 0.78*	34.16 ± 0.95	8.13 ± 1.03	7.96 ± 0.54
56 HFD-P (n=3)	24.1 ± 0.5	50.69 ± 0.8*	49.93 ± 0.1	9.93 ± 0.5	10.56 ± 0.28
56 HFD-L (n=3)	24.96 ± 0.78	54.56 ± 1.58*	52.52 ± 0.72	9.56 ± 0.53	7.26 ± 0.24 **

P: placebo; L: liraglutide; RD: regular diet; HFD: high-fat diet; 16, 32, 56: weeks of diet; BW: body weight; FBG: fasting blood glucose; *p<0.001 (BW before treatment *vs.* initial BW); ** P<0.05 (FBG pre *vs.* post treatment); ND: Not determined.

Supplemental Table 3: Echocardiography

Groups (n=10 each)	**HR** (bpm)	**EF** (%)	**FS** (%)	**LVIDd** (mm)	**LVIDs** (mm)	**IVS** (mm)	**LVPW** (mm)
32RD	548±16	78.4±1.2	41.4±1.2	4.38±0.12	2.57±0.08	0.70±0.02	0.76±0.02
32HFD Pre-L	612±34	62.6±1.4*****	30.3±0.7*****	4.07±0.1	2.90±0.08	0.72±0.03	0.83±0.04
32HFD Post-L	573±18	78.2±3.7$^{\#}$	42.1±1.5$^{\#}$	4.60±0.16	2.67±0.16	0.7±0.02	0.81±0.05

32RD, 32 weeks of regular diet;32HFD, 32 weeks of high fat diet; L, liraglutide; HR, heart rate; EF, ejection fraction; FS, fractional shortening;; LVIDd, left ventricular internal diameter in diastole; LVIDs, left ventricular internal diameter in systole; IVS, interventricular septum (thickness); LVPW, left ventricular posterior wall (thickness); 1-way ANOVA: *p<0.05 compared to RD; #p<0.05 *vs.* HFD post-L by Tukey multiple comparison *post-hoc* test.

Supplemental Table 4: Primer Sequences used for qRT-PCR:

Gene		**Sequence (5'-3')**
α-MHC	Forward	GCCAACCTGGAGAAAGTGTC
	Reverse	GCTGGGTGTAGGAGAGCTTG
β-MHC	Forward	GAGACGGAGAATGGCAAGAC
	Reverse	GATCATCCAGGAAGCGTAGC
ANP	Forward	CCGATAGATCTGCCCTCTTG
	Reverse	GCAGAATCGACTGCCTTTTC
BNP	Forward	GGTGCTGTCCCAGATGATTC
	Reverse	CCTTGGTCCTTCAAGAGCTG
GAPDH	Forward	AACTTTGGCATTGTGGAAGG
	Reverse	CACATTGGGGGTAGGAACAC

SUPPLEMENTAL FIGURE LEGENDS:

***Supplemental Figure 1*. Cardiac structure was not altered by 16 weeks of HFD; Cardiac GLP-1R levels are not affected by 16 or 32 weeks of HFD or liraglutide; Cardiac ANP levels are increased at 32 weeks of HFD.** (**A**) Heart sections (6 μm) from mice fed RD or HFD for 16 weeks were stained with Masson's trichrome (collagen is green) to assess levels of fibrosis and cardiomyocyte size. Representative transverse and longitudinal sections are shown. (**B**) Cardiomyocyte size was calculated by measuring the average cross-sectional surface area of 100 cardiomyocytes per section in 6 sections per animal with 5 animals per treatment group, expressing the result as a percentage of the average cross sectional area of the RD-fed controls (P=NS). (**C**) Western blot for ANP was performed using left ventricular protein extracts from RD- and HFD-fed mice at 16 and 32 week time points. Western blot for GAPDH was used as a loading control. L: liraglutide; P: placebo. While no different at 16 weeks of HFD (p=NS), cardiac ANP levels were elevated in mice fed HFD for 32 weeks; *$p<0.05$, N=3/group, unpaired Student's t-test.

Supplemental Figure 2: **Liraglutide increased Akt phosphorylation in lean mice, and increased expression of ER-stress response proteins; Neither obesity nor liraglutide affected XBP1 splicing or mitochondrial proteins; Liraglutide increased expression of an autophagy marker**. Treatment with liraglutide (L: 30 μg/kg/bid sc x 1 week) enhanced expression of phosphorylated Akt in hearts of RD-fed mice (**A**). H&E-stained liver sections from mice fed RD or HFD for 32 weeks revealed significant steatosis (lipid droplets, magnification 200X) (**B**). No evidence of XBP1 splicing was detected in the liverof these same HFD-fed mice, with no effect of liraglutide. Positive control for XBP1 splicing ismouse islets treated with thapsigargin (Tg) for 1 h (**C**). Liraglutide enhanced expression of ER associated markers, GRP 78/94 and PDI in the hearts of mice on HFD for 16 weeks (**D**). Neither 32 weeks of HFD nor liraglutide affect the cardiac abundance of mitochondrial related proteins PGC-1alpha, COX-IV and cyto C. Representative Western blots are shown (N=3 animals per group) (**E**). Treatment with liraglutide (L) increased cardiac expression levels of the autophagy marker LC3B-II in 32HFD-fed obese mice *vs*. 32RD and placebo (P)-treated 32HFD controls (**F**); Data are mean±SE; N=3 animals/group; 1-way ANOVA: * $p<0.05$ *vs*. RD-P, # $p<0.05$ *vs*. HFD-P, by Tukey multiple comparison *post-hoc* test.

Supplemental Figure 3: **A GLP-1 analogue modified human endothelial and monocyte cell interactions.** Treatment of TNFα-activated monolayers of HUVEC with GLP-1(7-36) (100 nM) reduced the number of human monocytes that subsequently attach to the endothelial monolayer. The GLP-1R antagonist Ex(9-39) abolished this anti-inflammatory action of GLP-1. Liraglutide (100 nM) also inhibited adhesion of THP-1 cells to TNFα-activated HUVEC. 1-way ANOVA: *$p<0.05$ *vs.* TNF-α-treated cells by Tukey multiple comparison *post-hoc* test.

Supplemental Figure 4: **Effects of GLP-1R activation on lipotoxicity models in cardiomyocytes and smooth muscle cells.** Mouse neonatal cardiomyocytes were treated with palmitic acid (PA, 250 nM) for 18 h. PA induced cellular swelling and cytoskeletal disintegration (green). Treatment with liraglutide (L, 100 nM) prevented these changes, an effect abolished by the GLP-1R antagonist Ex(9-39) (**A**). Assessment of apoptosis by Western blot for the active form of caspase-3 confirmed morphologic findings (**B**). Liraglutide (L, 100 nM) was

also cytoprotective for human coronary SMC exposed to the same dose of PA for 24 h, as demonstrated by morphologic analysis (**C**) and the XTT cell viability assay (**D**). 1-way ANOVA: *p<0.001 by Tukey multiple comparison *post-hoc* test.

Supplemental Figure 5: **Putative mechanisms underlying the effects of a GLP-1R agonist in obesity-induced heart disease.** Abbreviations: AMPK, AMP-activated protein kinase; Cx-43, connexin-43; eIF2α, eukaryotic translation initiation factor 2α; eNOS, endothelial nitric oxide synthase; ER, endoplasmic reticulum; ERK, extracellular signal-regulated kinase; GLP-1, glucagon-like peptide-1; GRP, Glucose-regulated protein; GSK-3β, glycogen synthase kinase-3beta; LC3-IIb, microtubule-associated protein-1 light chain-3 beta; NFκB p65, p65 subunit of the nuclear-factor kappa B; PDI, disulfide isomerase; pro-Col 1A1, collagen α1-type 1; TNF-α, tumor necrosis factor alpha.

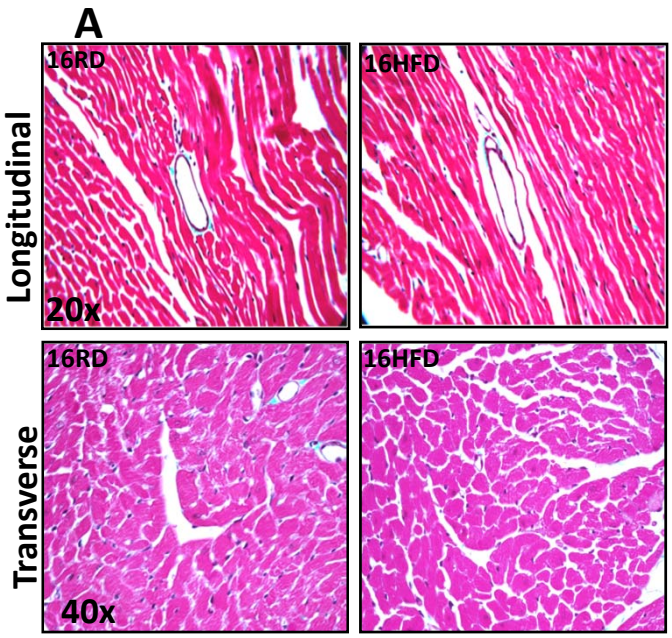

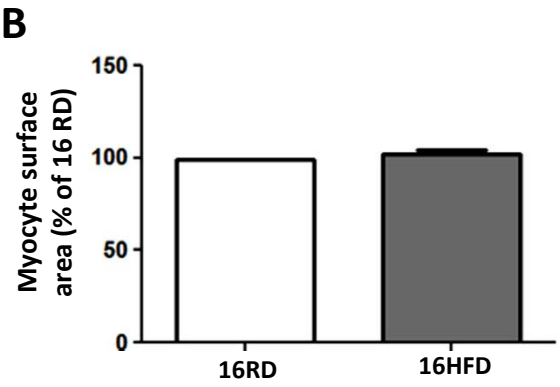

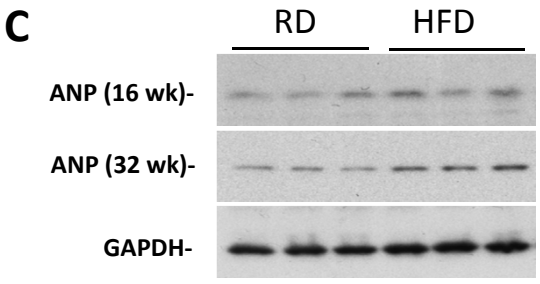

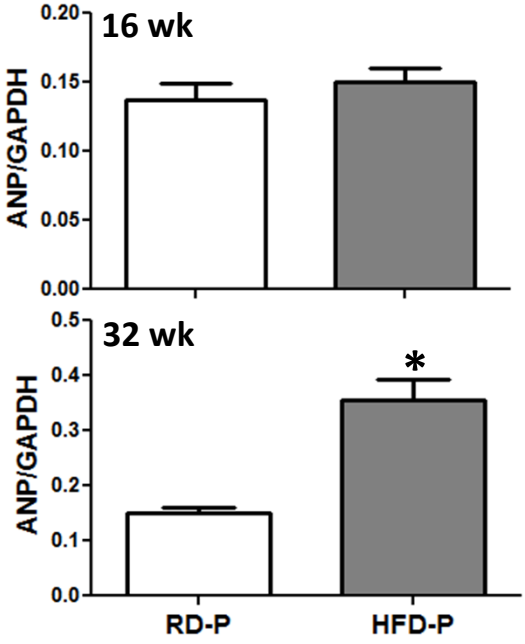

Supplemental Figure 1

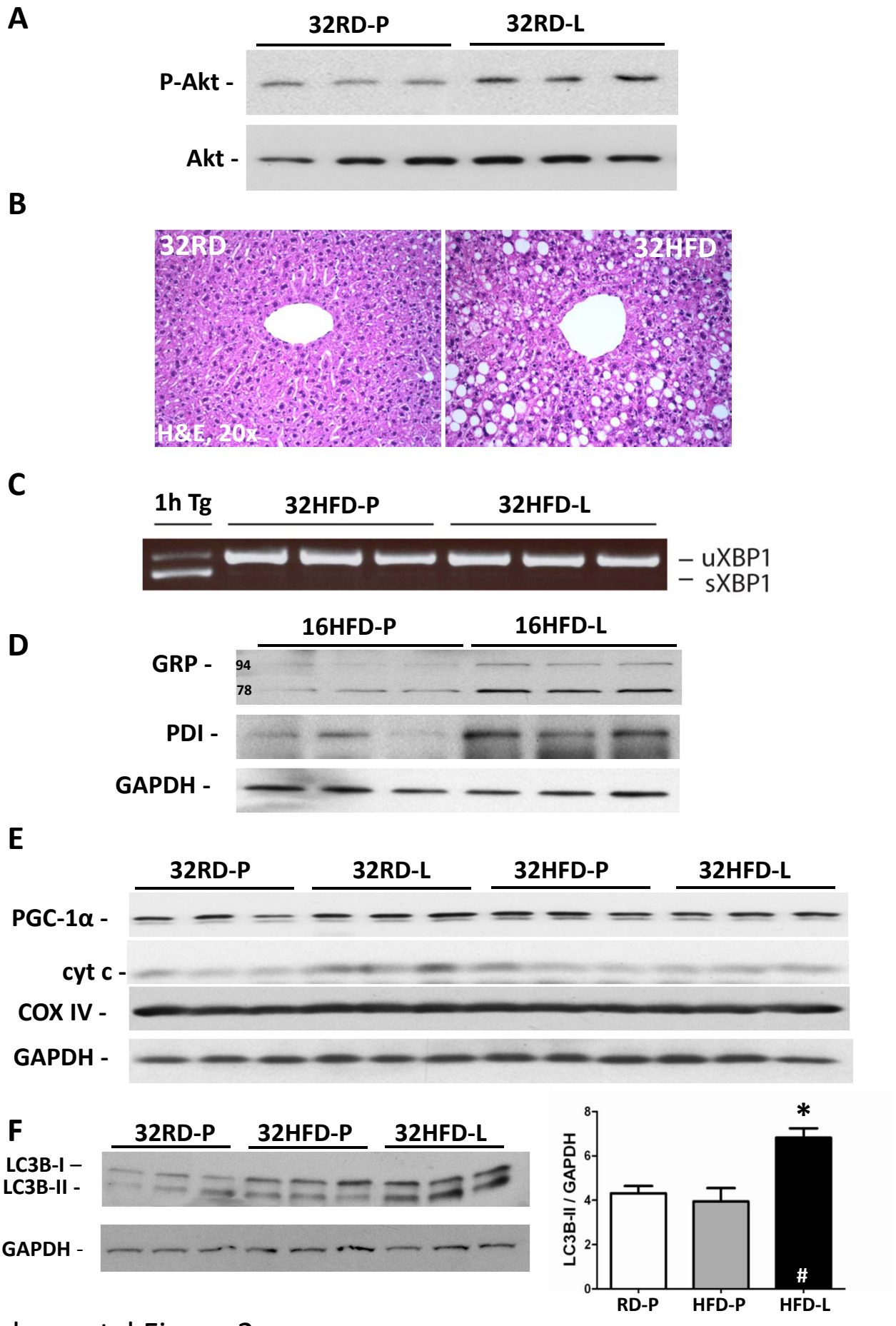

Supplemental Figure 2

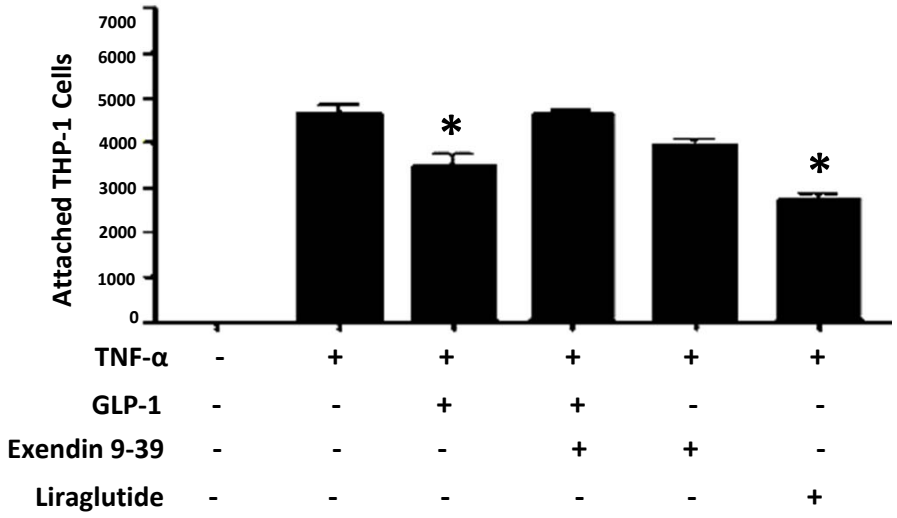

Supplemental Figure 3

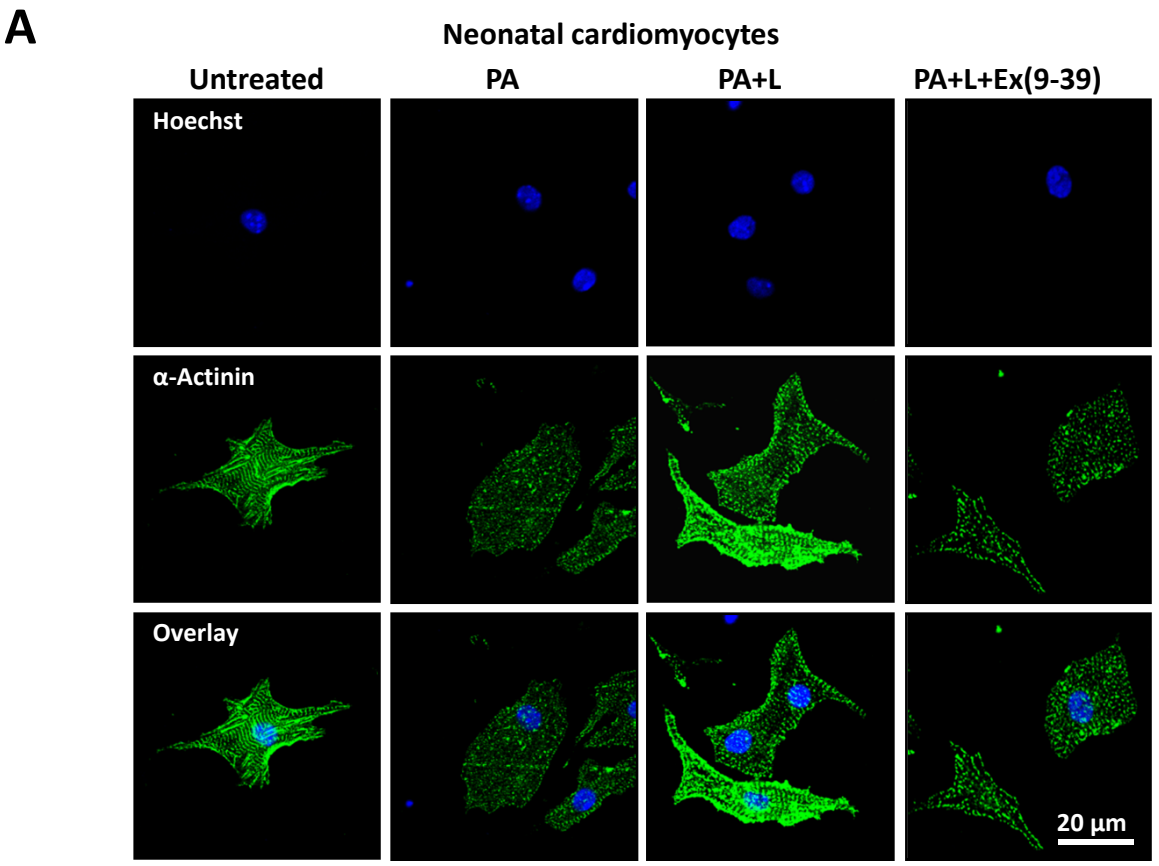

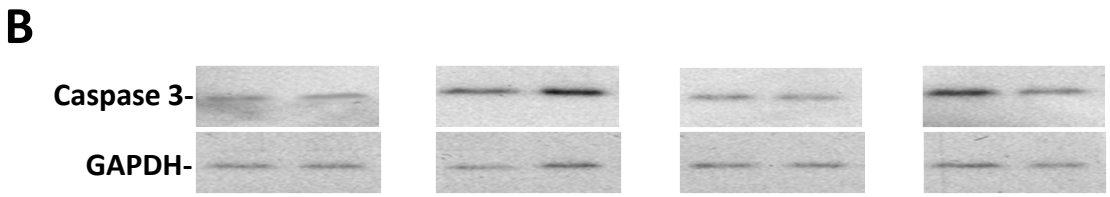

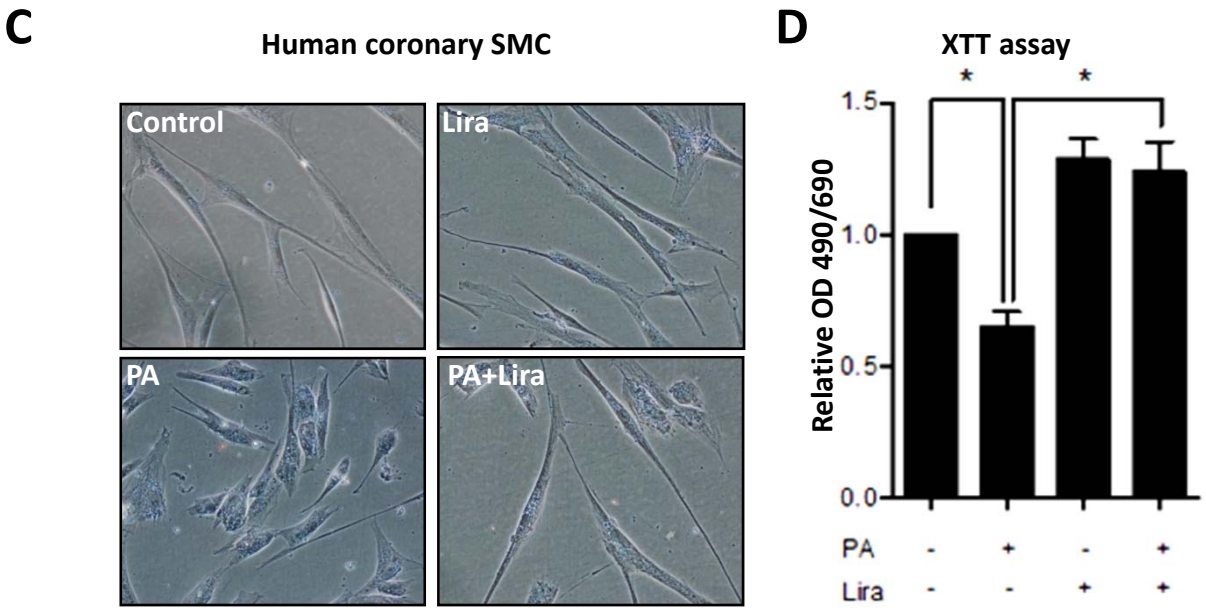

Supplemental Figure 4

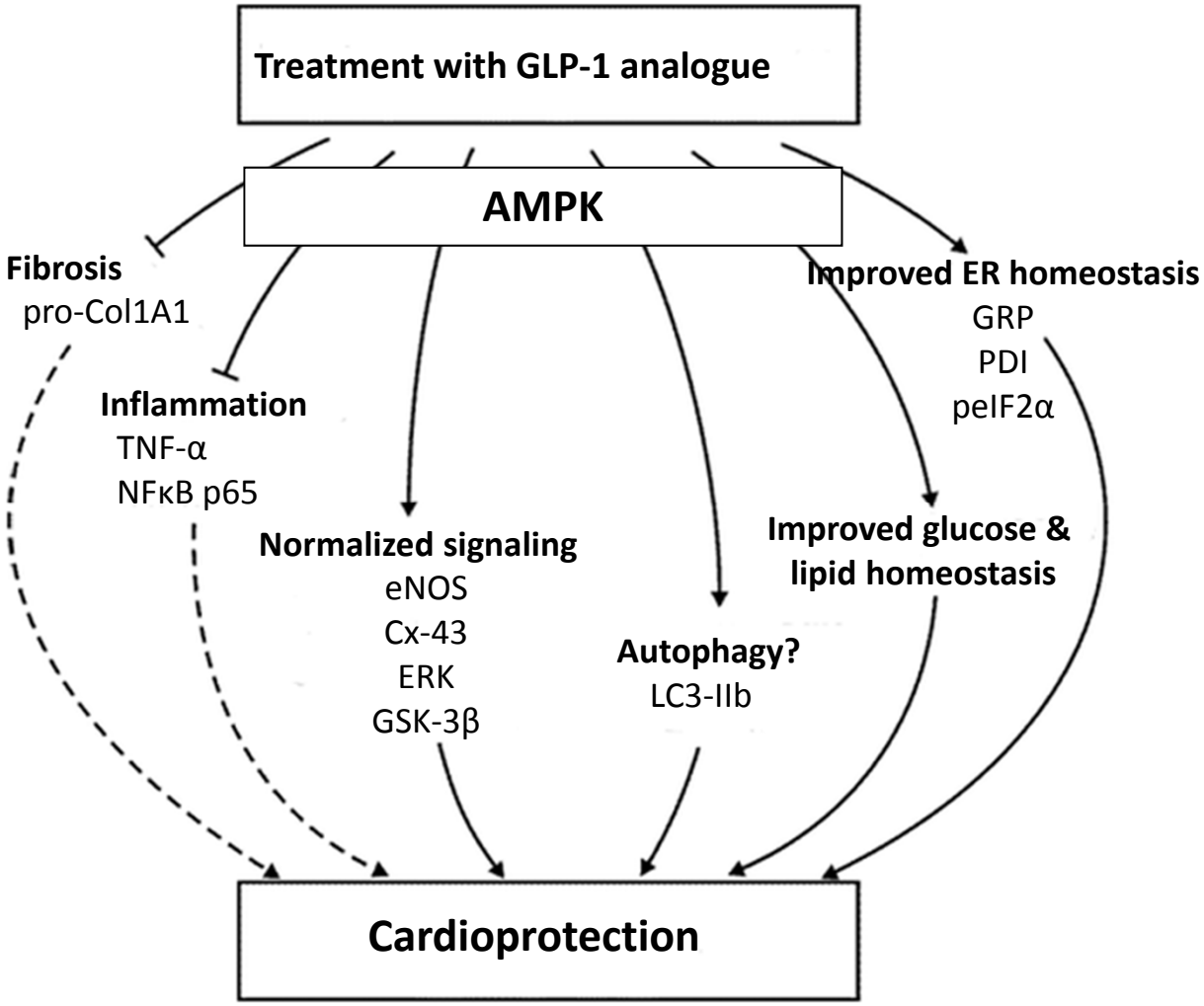

Supplemental Figure 5